



# Implementation and integration of slip and traction controllers for a three-wheel electric vehicle

Blanca Zumárraga



**LUND**  
UNIVERSITY

Department of Automatic Control

MSc Thesis  
TFRT-6182  
ISSN 0280-5316

Department of Automatic Control  
Lund University  
Box 118  
SE-221 00 LUND  
Sweden

© 2022 by Blanca Zumárraga. All rights reserved.  
Printed in Sweden by Tryckeriet i E-huset  
Lund 2022

# Abstract

The purpose of the Master Thesis is, on one hand, to develop a traction control system, integrating and implementing two controllers in the vehicle, each of them previously designed and tested separately, to test them together to evaluate their performance. On the other hand, to develop accurate and well-performing controllers, the data acquisition needs to be precise so parameters and devices need to be tuned again, because of small modification in the structure of the vehicle. Parameters such as the cornering and longitudinal stiffness were studied to have more faithful simulations, and devices such as the gyroscope and the ABS were tuned. Moreover, along the lines of acquiring accurate data, another purpose of the Master Thesis is to develop procedures or algorithms to acquire data using automated approaches, instead of the manual approaches that were used previously, specifically concerning the wheel's angles.

A mathematical representation of the vehicle dynamics, developed by [Nilsson and Sandstedt, 2021], is used to simulate the performance of the controllers and to tune them accordingly. Simulations were carried out to test the integration of the controllers and evaluate their performance. The controllers behaved according to the expectations and performed accurate simulations. The controllers should then be implemented in the real vehicle to confirm that their performance is the desired.

The data acquired provided information of each of the studied parameters and they showed that the procedure developed to obtain the wheel's angles was properly implemented. The devices that needed tuning were properly tuned. The model parameters were updated with new values so that the model represented the real system as well as possible.



# Acknowledgements

I want to thank, first of all the CEO of OMotion, Ola Svensson, for welcoming me in his company with open arms and his will to help me in the development of the work. Driving the OMotion2 was an amazing experience that I will not forget. Also, I want to thank my supervisors Björn Olofsson and Anders Robertsson for all the help and feedback provided. Lastly, I will like to thank Tore Hägglund, the examiner, for being interested in my work. I also want to wish him good luck in his new journey away from the academic world and to congratulate him on such a prolific career.





# Contents

|  |           |
|--|-----------|
| <b>List of Tables</b>                              | <b>9</b>  |
| <b>List of Figures</b>                             | <b>10</b> |
| <b>1. Introduction of the Project</b>              | <b>12</b> |
| 1.1 Objectives . . . . .                           | 13        |
| <b>2. Context</b>                                  | <b>14</b> |
| 2.1 OMotion . . . . .                              | 15        |
| 2.2 Electronic Stability Controls . . . . .        | 16        |
| 2.3 Traction Control Systems . . . . .             | 17        |
| 2.4 Model . . . . .                                | 18        |
| 2.5 Suspension . . . . .                           | 22        |
| <b>3. Methodology</b>                              | <b>25</b> |
| 3.1 Motivation . . . . .                           | 25        |
| 3.2 Process . . . . .                              | 25        |
| 3.3 Resources and Tools . . . . .                  | 29        |
| <b>4. Front Wheel Alignment</b>                    | <b>31</b> |
| <b>5. Device and Model Parameters Tuning</b>       | <b>37</b> |
| 5.1 Gyroscope and Accelerometer . . . . .          | 37        |
| 5.2 ABS . . . . .                                  | 38        |
| 5.3 Steering Wheel Sensor . . . . .                | 39        |
| 5.4 Cornering and Longitudinal Stiffness . . . . . | 39        |
| 5.5 Dimensions of the Vehicle . . . . .            | 40        |
| 5.6 Current to Torque Conversion . . . . .         | 40        |
| 5.7 Filtering . . . . .                            | 42        |
| <b>6. Model</b>                                    | <b>43</b> |
| <b>7. Controllers</b>                              | <b>48</b> |
| 7.1 Slip Control . . . . .                         | 48        |
| 7.2 Traction Control . . . . .                     | 50        |
| 7.3 Integration . . . . .                          | 52        |
| 7.4 Tuning . . . . .                               | 53        |

|  |           |
|--|-----------|
| <b>8. Simulation</b>                       | <b>54</b> |
| 8.1 Integration of Controllers . . . . .   | 54        |
| <b>9. Implementation</b>                   | <b>65</b> |
| 9.1 Front Wheel Suspension . . . . .       | 65        |
| 9.2 Current to Torque Conversion . . . . . | 66        |
| <b>10. Experiments and Results</b>         | <b>67</b> |
| <b>11. Conclusion</b>                      | <b>73</b> |
| 11.1 Future Work . . . . .                 | 74        |
| <b>Bibliography</b>                        | <b>75</b> |
| <b>A. Nomenclature</b>                     | <b>77</b> |
| <b>B. Sustainable Development Goals</b>    | <b>79</b> |

# List of Tables

|  |    |
|--|----|
| 8.1 Behaviour of controllers . . . . . | 54 |
| A.1 Nomenclature I . . . . .           | 77 |
| A.2 Nomenclature II . . . . .          | 78 |

# List of Figures

|     |  |    |
|-----|--|----|
| 2.1 | OMotion2 vehicle. Photo: OMotion AB . . . . .                            | 14 |
| 2.2 | OMotion. Photo: OMotion AB . . . . .                                     | 15 |
| 2.3 | OMotion2. Photo: OMotion AB . . . . .                                    | 17 |
| 2.4 | Camber angle . . . . .   | 23 |
| 2.5 | Caster angle . . . . .   | 23 |
| 2.6 | Toe angle . . . . .  | 24 |
| 4.1 | Coordinates systems for front wheel suspension . . . . .                 | 32 |
| 4.2 | Vector distribution for steady-state front wheel suspension . . . . .    | 33 |
| 4.3 | Strut force from vertical tyre force . . . . .                           | 34 |
| 4.4 | Wheel angle sign convention . . . . .                                    | 36 |
| 5.1 | Displacement between gyroscope and accelerometer coordinate system       | 38 |
| 5.2 | Current-to-torque ratio vs velocity . . . . .                            | 41 |
| 5.3 | Filtering of data used as input for computations . . . . .               | 42 |
| 6.1 | Block diagram of the inputs and outputs of the model . . . . .           | 44 |
| 6.2 | Block diagram of the model . . . . .                                     | 45 |
| 6.3 | Forces acting on the vehicle seen from the side . . . . .                | 46 |
| 6.4 | Forces acting on the vehicle seen from above . . . . .                   | 46 |
| 7.1 | Block diagram of the slip control . . . . .                              | 49 |
| 7.2 | Traction on-off control with hysteresis . . . . .                        | 51 |
| 7.3 | Traction on-off control with hysteresis . . . . .                        | 52 |
| 7.4 | Simple block diagram of the integration of the controllers . . . . .     | 53 |
| 8.1 | Slip ratio with slip control off and traction control off . . . . .      | 55 |
| 8.2 | Input torque with slip control off and traction control off . . . . .    | 55 |
| 8.3 | Yaw rate with slip control off and traction control off . . . . .        | 56 |
| 8.4 | Traction control mode with slip control off and traction control off . . | 56 |
| 8.5 | Slip control mode with slip control off and traction control off . . . . | 56 |

|      |  |    |
|------|--|----|
| 8.6  | Slip ratio with slip control on and traction control off . . . . .                           | 57 |
| 8.7  | Input torque with slip control on and traction control off . . . . .                         | 58 |
| 8.8  | Slip control mode with slip control on and traction control off . . . . .                    | 58 |
| 8.9  | Traction control mode with slip control on and traction control off . . . . .                | 58 |
| 8.10 | Slip ratio with slip control on and traction control on . . . . .                            | 59 |
| 8.11 | Input torque with slip control off and traction control on . . . . .                         | 60 |
| 8.12 | Traction control mode with slip control on and traction control off . . . . .                | 60 |
| 8.14 | Actual yaw rate and desired yaw rate with slip control off and traction control on . . . . . | 60 |
| 8.13 | Vehicle's speed with slip control off and traction control on . . . . .                      | 61 |
| 8.15 | Slip ratio with slip control on and traction control on . . . . .                            | 62 |
| 8.16 | Input torque with slip control on and traction control on . . . . .                          | 62 |
| 8.17 | Actual yaw rate and desired yaw rate with slip control on and traction control on . . . . .  | 63 |
| 8.18 | Traction control mode with slip control on and traction control on . . . . .                 | 63 |
| 8.19 | Slip control mode with slip control on and traction control on . . . . .                     | 63 |
| 10.1 | Vertical loads . . . . .   | 68 |
| 10.2 | Steering wheel angle . . . . .   | 68 |
| 10.3 | Wheel's angles . . . . .   | 69 |
| 10.4 | Camber angles . . . . .  | 70 |
| 10.5 | Strut lengths . . . . .  | 71 |
| 10.6 | Sip ratio provided by vehicle . . . . .  | 72 |
| 10.7 | Motor current of the vehicle . . . . .   | 72 |
| B.1  | Sustainable development goals. Photo: United Nations . . . . .                               | 79 |

# 1

## Introduction of the Project

Since the first vehicles were developed, the automotive industry has been challenged with safety issues to enhance the safety of the driver and the passengers of the vehicle. Traction control systems are safety systems part that are able to detect whether a loss of traction has happened while driving and in the case that it does, it acts automatically to brake or cut down the power of the wheel that is suffering the loss of traction. This Master Thesis develops the existing knowledge about how control theory has a major impact on vehicles nowadays, using it to further improve the safety of those inside the vehicle with automated control systems. This Master Thesis is based on the work of [Nilsson and Sandstedt, 2021] and [Karlin, 2021].

OMotion AB is a Swedish start-up that designs and manufactures three-wheel electric vehicles [OMotion, 2021]. An empirical field investigation was carried out with the aim of improving the safety of the vehicle during driving through the further development of a traction control System (TCS). This is the main focus of the Master Thesis. Using controllers developed by previous Master Theses, the aim of this Master Thesis is to integrate them, implement them in the vehicle and test them on the real vehicle to evaluate the performance, as the controllers have previously only been tested separately. To develop a traction control system, the data that is going to be analysed by the control needs to be accurate. The vehicle initially had procedures to acquire data that were done manually or in a non-optimal way. The aim is to find process or algorithms that procure the data using automated approaches to obtain more precise and realistic values. One of these procedures is the calculation of the wheel's angle values. It is key to be able to have real-time data from the wheel to design a precise control and to have an accurate model to perform accurate simulations. Another one of these procedures that was not optimal is the conversion of the current of the motor to torque. It was previously done using a constant factor, but after some tests, it was seen that the factor was affected by the vehicle's speed and that it changed dynamically. Moreover, the vehicle has seen some physical modifications and some parameters of the model needed to be tuned again as well as some devices that are part of the vehicle. Specifically, this concerned the gyroscope and accelerometer device and the cornering and longitudinal stiffness parameters. During the Master Thesis, more devices needed to be tuned

that were not thought of previously, such as the ABS and the steering wheel sensor. The process for tuning of the devices was developed by doing tests that provided updated parameters for each device.

To integrate both controllers, a model was used to simulate their behaviour. Once multiple simulations were run, it was concluded that the controllers worked as it was expected. The control parameters that were used on the simulations were the ones designed by the previous Master Thesis [Karlin, 2021] [Nilsson and Sandstedt, 2021] while the control logic parameters were modified.

To test that the procedures for the calculation of the wheel's angles were implemented properly, experiments were run, gathering data and contrasting the implemented data with data acquired from models.

## **1.1 Objectives**

At the beginning of the Master Thesis, the following objectives were set:

- Integrate and implement two controllers in the vehicle, each of them previously designed and tested separately, to test them together to evaluate their performance.
- Develop procedures or algorithms to acquire data using automated approaches, specifically for the wheel's angles and the conversion of current to torque.
- Tune parameters and devices of the vehicle because of small modifications in the structure, specifically the gyroscope and the accelerometer devices and the cornering and longitudinal stiffness parameters.
- Search for solutions to solve the difficulties in the tuning of the traction control parameters, searching for approaches to adapt the parameters of the control online.

# 2

## Context



**Figure 2.1** OMotion2 vehicle. Photo: OMotion AB

Since the first vehicles were developed, the automotive industry has been challenged with safety issues to enhance the safety of the driver and the passenger of the vehicle. Vehicles are now seen as electromechanical machines instead of purely mechanical. Nowadays vehicles have many different mechanical and electronic components such as sensors, actuators, microprocessors and actuators, among other things, which are used to further improve safety and fuel consumption. Thanks to the technology available, sensors have been designed to acquire valuable information that is used to know whether the vehicle is performing as it should, given the



driver's input, and act accordingly in a situation where the performance is not adequate. This is known as electronic stability controls [Rajamani, 2012a], and from now on referred to as ESC.

In the academic world, there are many researchers that have put their focus on developing traction controls for different vehicles such as motorbikes, four-wheel cars and trucks. In [Kachroo and Tomizuka, 1994], the authors mention the different applications that exist nowadays where traction control is being used. As there are many different control strategies available, there are many topics of research in this field. [Jalali, Khajepour, Chen and Litkouhi, 2016] uses an MPC strategy to develop a traction control for electric vehicles, while [Kawabe, 2012] used a predictive PID to develop a traction control system for electric vehicles.

## 2.1 OMotion



**Figure 2.2** OMotion. Photo: OMotion AB

OMotion AB is a Swedish start-up that designs and manufactures three-wheel electric vehicles[OMotion, 2021], see Figure 2.1 and 2.3. It was founded in 2013 by Ola Svensson and currently, a second version of the first vehicle is being manufactured. It is a high-quality, safe and light vehicle. The company has designed their own electric control unit and from now on referred to as ECU, which is a device that controls all the electronic and digital aspect of the behaviour of the vehicle. This allows them to have customised control over the behaviour and performance of the vehicle.

OMotion has also developed an app for users that allows them to have a better knowledge of the vehicle's conditions and also enables the company to update the vehicle's software system whenever there is a new update. The first working vehicle was completed a couple of years ago and since then, they have been improving the features of the vehicle. One of the points where OMotion has put its focus in the past year and present year is in improving safety while driving, developing its own traction control system (TCS). The work that was carried out in this thesis is related

to the development of the TCS and is based on the work of [Karlin, 2021] and [Nilsson and Sandstedt, 2021], students from Lund University that worked for OMotion in the past year developing a slip control and a traction control, respectively, both relevant parts of the TCS. Their work was to design, implement and test the controllers separately and evaluate their performance. The work done in the previous theses was carried out using OMotion ETR, the first working vehicle of OMotion. Now, OMotion has developed a second version of the vehicle, called OMotion2. This is the vehicle was used. The vehicles have some differences between them, such as the dimensions of certain parts or structures.

The vehicle is an electric light three-wheeler aimed to be used for recreational and short commuting distances for two people, as Figure 2.1 and Figure 2.3 show. The second version, OMotion2, the vehicle that was used in the Master Thesis, was released in the summer of 2021. It provided new and improved features compared to its predecessor. There are two front wheels and one rear wheel. The length of the vehicle is 2.78 m, the width of the vehicle is 1.66 m and the height is 1.12 m, with a total weight of 370 kg. It is equipped with a 72 V Lithium NMC (Nickel Manganese Cobalt) battery with 11.2 kW per hour capacity that provides a range of 150 km. The maximum speed that OMotion2 can provide is 110 km/h. The motor is located in the rear wheel and provides 24 kW peak and 11 kW continuous power. This means that the rear wheel is the driving wheel while the front wheels are not. The speed of the rear wheel is the speed of the motor, as there are no gears. It is equipped with ABS brakes and is can be driven on any European road as it meets the requirements. Depending on the country, it can be mandatory to use a helmet while driving it [OMotion, 2021].

## 2.2 Electronic Stability Controls

The ESC is a system that uses the information obtained by sensors and evaluate the data to see if the vehicle's behaviour is the desired [Rajamani, 2012a]. The breakthrough of ESC came with the development of the anti-lock braking system [Aly, Zeidan, Hamed and Salem, 2011] which from now on is referred to as ABS. The ABS is used in vehicles to help the driver maintain control of the vehicle in dangerous braking situations avoiding the lock of the wheels while braking, so that sliding situation are avoided [Aly, Zeidan, Hamed and Salem, 2011]. The ESC's aim is to improve the safety of the vehicle by acting automatically when an undesired situation arises, using data from different sensors, analysing it using control strategies and acting accordingly to bring the vehicle back to a stable situation. Many automotive companies have developed their own ABS and ESC systems. Having an own ESC allows the manufacturers to customize the system. This is the case with OMotion. To make the vehicle safer, the company wants to develop their own ESC using control theory and the ABS features to give better performance under undesirable situations.



**Figure 2.3** OMotion2. Photo: OMotion AB

## 2.3 Traction Control Systems

One of the many different aspects of control theory in vehicles is the known TCS (traction control system). A TCS is a safety system part of the ESC that is able to detect whether a loss of traction has happened while driving and in the case that it does, it acts automatically to brake or cut down the power of the wheel that is suffering the loss of traction [Kachroo and Tomizuka, 1994]. Before going into detail explaining what TCS is, there are some concepts that need to be further explained, such as loss of traction and slip. A slip is an action of sliding during a short period of the time unintentionally [Kachroo and Tomizuka, 1994]. The slip of wheels is the action of having a spinning wheel without actually having a grip on the surface, meaning that the vehicle does not move while the wheels spin. A loss of traction is a situation where the wheel starts to slip and does not have the desired grip or no grip with the road. There are many cases when this situation can happen. The typical ones are when the driver pushes the throttle down really fast to accelerate the vehicle but the tyres do not have the friction capacity to have a grip on the road in that short period of time, so the wheels start spinning without having a grip on the road. The same occurs when a braking situation happens. The driver can push the brake pedal down really fast but the tyres cannot get a grip on the road because of the fast-changing speed and the wheels start to slip with the road. The slip in these two cases is known as longitudinal slip, as the slip occurs along the longitudinal

axis of the wheel. Another situation when traction is lost is while turning when the acceleration that the vehicle has is bigger than the one the vehicle needs to make a turn without slipping, so the vehicle starts to slip sideways against the direction of the turn. This slip is known as a lateral slip as the slip occurs mostly along the lateral axis of the wheels. From a mathematical point of view, a slip is an angular displacement between the actual direction of the vehicle and the direction the wheel is pointing to. A slip occurs when the value of the force that is applied to a tyre is bigger than the traction available to that tyre. There is a certain situation where a loss of traction is more likely to happen, for example, when the road has a low friction coefficient, such as snow, ice or wet roads. TCS has existed for decades in various forms but it was until 2011 that it became mandatory for manufacturers to include this feature in all new vehicles [Urda, Cabrera, Castillo and Guerra, 2016]. In the academic world, there have been many researchers that have discussed the importance and the improvements that traction control systems bring to the stability of the vehicle's performance, such as [Jo, You and Joeng, 2008]. In this article, the importance of TCS is stated not only regarding the safety aspects for the drivers but also regarding the performance of the vehicle using control strategies. It continues by pointing out that traction control improves vehicle stability and vehicle motion performance. Adequate traction control will prevent the driving wheels to slip if the driver mistakenly pushes down the acceleration pedal in a curve when the road condition are not the desired ones, just by automatically controlling the wheel slip. Moreover, [Decker, Emig and Schramm, 1987] makes a statement regarding the importance of the ABS system in TCS, as they mention the positive aspect that ABS had when it was introduced.

## 2.4 Model

To develop a good and working controller, a mathematical model that represents the real system is beneficial. Models are basically a tool that is used to investigate real engineering problems. Is a mathematical representation of a real system [Crouch and Haines, 2004]. It can represent something that already exists or in some cases, models are used as a design tool. A model can be used to investigate if the performance of an existing machine changes when a control strategy is added. On the other hand, a model can be used to investigate what could be the output of a system when the input variables change, for example, how the workflow of a warehouse will be affected when the volume of orders changes. Models are really useful because they are cost-effective and time-effective tools used to analyse the design solution in real-world conditions and to evaluate if it can improve the system's performance. Usually, models are easier and faster to build than the real system. In the case of this Master Thesis, a model is used to mimic the dynamic behaviour of OMotion2. To create a model, mathematical algorithms need to be used to represent the motion of the vehicle. In the academic world, there are many researchers

that have put their focus on making a mathematical representation of the dynamics of the vehicle, such as [Rajamani, 2012b] and [Gillespie, 1992]. To model the vehicle's motion, there are multiple aspects that need to be taken into account. The performance of the tyres is of utmost importance. [Pacejka, 2012] describes in his book the dynamics of the tyres and the different approaches to developing control systems. Modern control strategies are currently being used in the automotive sector to provide additional safety and to optimize fuel consumption. [Athans, 1978] predicted in his article the relevance that modern control strategies would have in the automotive sector. Depending on how much accuracy is wanted in the model and what is being researched, the vehicle's behaviour can be modelled with many different approaches.

### Nilsson and Sandstedt Model

The model that was used was created by [Nilsson and Sandstedt, 2021]. In their work, they used vehicle dynamic equations described in [Rajamani, 2012b], as well as [Dugoff and Segel, 1969] for the tyre dynamics.

The aim of the model is to represent the vehicle's dynamic behaviour. While driving, the vehicle dynamics are strongly affected by forces acting on the wheels, aerodynamic forces, rolling resistance forces and load forces. The calculation of these forces to calculate the velocity of the vehicle falls back under the area of vehicle dynamics. A classification of these forces is made, depending on the axis along which they are acting. Longitudinal forces group all the forces that act along the longitudinal axis of the vehicle, known as well as the x-axis, and lateral forces group all the forces acting on the lateral axis of the vehicle, known as well as the y-axis. The rolling resistance, the aerodynamic force and the longitudinal tyre force make the longitudinal force while the lateral tyre force, additional chassis and suspension forces make the lateral force. Lateral forces play a very important part when the vehicle is cornering [Rajamani, 2012b].

The rolling resistance force is a **force that opposes the motion of a body when is rolling on a surface**, from now on referred to as  $F_{rr}$ . [Rajamani, 2012b] describes the force using Equation (2.1) when the sum of normal forces in the vehicle is equal to the mass ( $m$ ) multiplied by the gravity ( $g$ ) and the rolling resistance coefficient, from now on referred to as  $C_r$ , is equal for both tyres. With these assumptions, the force can be simplified to a sole force, instead of having a force acting on each wheel. The rolling resistance  $F_{rr}$  is given by

$$F_{rr} = C_r mg \quad (2.1)$$

where  $m$  is the mass of the vehicle,  $g$  is the gravity force and  $C_r$  is the rolling resistance coefficient. The aerodynamic force acting on the vehicle is known as the air resistance force, which from now on is referred to as  $F_d$ . It is a **force opposing the motion of a body when it moves through air**. [Rajamani, 2012b] describes the force using Equation (2.2). It takes into account the density of the air, the frontal

area of the body that is moving, the velocity of the body and a coefficient that measures the resistance of the body in a fluid environment. This coefficient value varies depending on the body dimension and have been deeply researched throughout the years. The aerodynamic forces is given by

$$F_d = \frac{\rho \dot{x}^2 C_d A}{2} \quad (2.2)$$

Where  $\rho$  is the density of the air,  $C_d$  is the drag coefficient and  $A$  is the frontal area of the vehicle.

The forces acting on a wheel or tyre are the longitudinal tyre force, referred to as  $F_x$ , the lateral tyre force, referred to as  $F_y$ , and the vertical tyre force, referred to as  $F_z$ . Dynamically, these forces will change as a result of the speed of the vehicle and cornering, among other things. Research has mentioned the importance of accuracy in the development of accurate mathematical representations of these forces. [Rajamani, 2012b] explains different mathematical procedures to calculate these forces depending on the approach that is adopted. Some existing approaches for lateral dynamics are the dynamic bicycle model, the dynamic model in terms of error with respect to the road and the dynamic model in terms of yaw rate and slip angles. Approaches for longitudinal dynamics take into account the slip ratio concept, which is explained in at the end of this section. There are also different approaches for tyres that have both lateral and longitudinal forces acting on the wheels. Some approaches for the calculation of lateral and longitudinal forces when both are present are the Magic Formula tyre model [Pacejka, 2012], Dugoff's tyre model [Dugoff and Segel, 1969] and the dynamic tyre model. The Dugoff's tyre model is going to be explained as it was the model chosen by the previous Master Thesis [Nilsson and Sandstedt, 2021] [Karlin, 2021]. It is an analytical model that calculates a normalized lateral slip and longitudinal slip and then calculates the normalized global slip as follows:

$$\bar{\sigma} = \frac{\sigma C_\sigma}{\mu F_z (1 - \sigma)} \quad (2.3)$$

$$\bar{\alpha} = \frac{\tan(\alpha) C_\alpha}{\mu F_z (1 - \sigma)} \quad (2.4)$$

$$\bar{\sigma}_r = \sqrt{\bar{\sigma}^2 + \bar{\alpha}^2} \quad (2.5)$$

where  $\sigma$  is the longitudinal slip ratio,  $\alpha$  is the slip angle of the wheel,  $C_\sigma$  is the tyre longitudinal stiffness,  $C_\alpha$  is the tyre cornering stiffness,  $\mu$  is the friction coefficient between the tyre and the road and  $F_z$  is the normal force on the tyre.  $\bar{\sigma}$  is the normalized longitudinal slip ratio,  $\bar{\alpha}$  is the normalized lateral slip ratio and  $\bar{\sigma}_r$  is the normalized global slip ratio.

The resultant slip is then used to calculate a normalised tyre force

$$F = \begin{cases} \mu F_z \bar{\sigma}_r, & \text{if } \bar{\sigma}_r < 0.5 \\ \mu F_z (1 - \frac{1}{4\bar{\sigma}_r}), & \text{if } \bar{\sigma}_r \geq 0.5 \end{cases} \quad (2.6)$$

Once this force is obtained, the model splits the force into longitudinal force and lateral force.:

$$F_x = \frac{\bar{\sigma}}{\bar{\sigma}_r} F \quad (2.7)$$

$$F_y = -\frac{\bar{\alpha}}{\bar{\sigma}_r} F \quad (2.8)$$

As mentioned before, OMotion2 has three wheels, two wheels on the front axis and one on the rear. The vehicle is rear-wheel driven, so that means that the torque is only applied to the rear wheel. Braking is applied on all three wheels. Wheel dynamics can be obtained according to [Rajamani, 2012b] as

$$I_{wf} \dot{\omega}_{fl} = -\tau_{bfl} - r_f F_{xfl} \quad (2.9)$$

$$I_{wf} \dot{\omega}_{fr} = -\tau_{bfr} - r_f F_{xfr} \quad (2.10)$$

$$I_{wr} \dot{\omega}_r = \tau - \tau_{br} - r_r F_{xr} \quad (2.11)$$

where  $I_{wf}$  and  $I_{wr}$  are the moment of inertia for the front wheels and the rear wheel respectively.  $\dot{\omega}_{fl}$ ,  $\dot{\omega}_{fr}$  and  $\dot{\omega}_r$  are the angular acceleration of the front wheels and the rear wheel.  $\tau$  is the torque from the motor acting on the rear wheel.  $\tau_b$  is the braking torque.  $F_{xfl}$ ,  $F_{xfr}$  and  $F_{xr}$  are the longitudinal forces acting on the front wheels and the rear wheel, respectively. Lastly,  $r_f$  and  $r_r$  are the outer radius of the front wheel and the rear wheel respectively. [Pacejka, 2012] and [Friedrich, 2014] mention in their work an important parameter that affects the dynamics of the wheels. This parameter is the slip ratio. When the value of the force that is applied to a tyre is bigger than the traction available to that tyre, the wheels slip. This situation mostly occurs when cornering or when the acceleration or braking of the tyres is sudden. To take this occurrence into account, the slip ratio is described by [Rajamani, 2012b], among others, with Equation (2.12) for acceleration and with Equation (2.13) for braking. For the former, the slip ratio is the **ratio between the difference in the velocity of the tyre and the linear velocity of the vehicle and the velocity of the tyre**. For the latter, the slip ratio is the **ratio between the same difference and velocity of the vehicle**. The longitudinal slip affects the longitudinal forces primarily, as [Rajamani, 2012b] explains in his work. The slip ratios are given by

$$\sigma_a = \frac{\omega r_r - \dot{x}}{\omega r_r} \quad (2.12)$$

$$\sigma_b = \frac{\omega r_r - \dot{x}}{\dot{x}} \quad (2.13)$$

where  $\sigma_a$  and  $\sigma_b$  are the slip ratio when acceleration and braking respectively,  $\omega$  is the angular velocity of a wheel,  $r_r$  is the radius of the wheel and  $\dot{x}$  is the linear velocity of the vehicle.

## 2.5 Suspension

A suspension is a group of elements that link the wheels of the vehicle with the chassis [Furferi, Governi, Volpe and Carfagn, 2013]. The suspension structure allows a relative movement between the chassis and the wheels. The aim of the suspension in vehicles is the following: if a bump is encountered while driving, the suspension structure will take most of the hit while the chassis will take a lesser hit. This way, the elements on the chassis of the vehicle, the driver and the passengers do not suffer the irregularities of the road. The suspension provides stability to the vehicle while driving as well as comfort to the passengers. Companies have developed their own suspension structure, so there are many different types. Once the suspension structure is designed and built, wheel alignment is required to set all the elements in their correct position and dimensions. The front-wheel suspension structure is dictated by the front wheel alignment and has a strong impact on the performance of the vehicle.

The wheel alignment structure is associated with a group of parameters whose values define the behaviour of the dynamics of the vehicle. There are plenty of parameters that impact the wheel alignment, but only the most relevant are going to be discussed here. These parameters are the ground clearance, the camber angle, the caster angle and the toe angle.

The camber the angle is the displacement measured in degrees between the vertical axis of the coordinate system and the vertical axis of the wheel, see Figure 2.4 shows [Pundir, 2019]. This displacement has been shown to improve the performance of the vehicle when cornering, braking and acceleration among others. It can have either positive or negative values. When the wheel is tilted outwards, the camber angle is positive, while when is tilted inwards, the camber angle is negative. The value of the camber angle changes dynamically while driving and mostly when cornering. Negative nominal camber angles are used in racing cars, to have a better grip when cornering, while positive nominal values are used for passenger cars, to, for example, compensate when the car is fully loaded, as it will become zero. The value of the camber angle is strongly affected by many other parameters, such as the Kingpin inclination, known as KPI, the wheel's angles, the caster angle and the direction the vehicle is cornering (right or left) [Furferi, Governi, Volpe and Carfagn, 2013].

The caster is the displacement measured in degrees between the kingpin axis and the vertical axis of the vehicle, seen from the side, as Figure 2.5[Pundir, 2019]. As the camber, the value of this displacement has an impact on the vehicle's performance. The caster can be positive or negative. When the lower kingpin endpoint is in front of the upper endpoint, the caster is positive, while when the upper endpoint is in front of the lower endpoint, the caster is negative. Positive values improve the stability of the vehicle when driving straight and improve the performance when cornering. A negative caster angle does not give many advantages, being the most relevant is that the steering structure requires less effort to make a steering. The



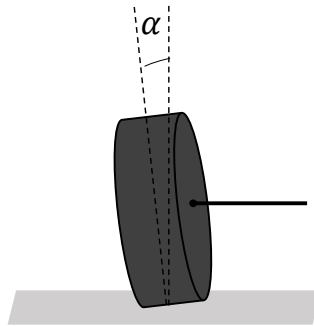


**Figure 2.4** Camber angle

value of the caster angle also changes dynamically, but to a lesser extent compared to the camber angle [Furferi, Governi, Volpe and Carfagn, 2013].

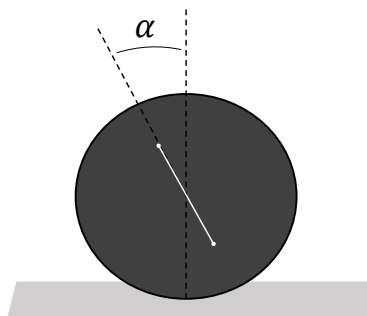


**Figure 2.5** Caster angle

The toe is the displacement measured in angles between the wheel's longitudinal axis and the longitudinal axis of the vehicle, as Figure 2.6 shows [Pundir, 2019]. Its value also affects the behaviour of the vehicle. It can either be positive or negative. When the wheels are facing inwards, the toe is positive and this is known as toe-in. When the wheels are facing outwards, the toe is negative and it is known as toe out. Positive values increase the understeer of the vehicle while negative values increase the oversteer. The value of the toe angle does not change dynamically but the wheel's angle depends on this parameter, among other things [Furferi, Governi, Volpe and Carfagn, 2013].

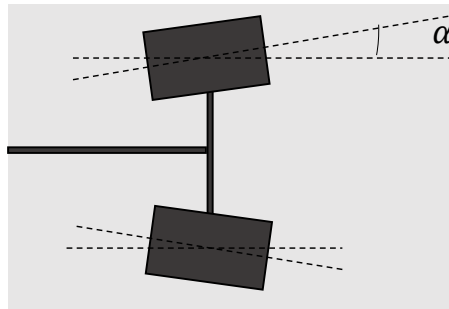


**Figure 2.6** Toe angle

Lastly, the ground clearance is a parameter that indicates the distance between the lowest point of the vehicle and the ground. The value of this parameter is key for the suspension system of the vehicle [Furferi, Governi, Volpe and Carfagn, 2013]. This value changes dynamically as the forces acting on the tyres vary while driving because of irregularities on the road or when cornering.

# 3

## Methodology

### 3.1 Motivation

Sweden has been one of the top countries in the secondary and service sector for over decades, with companies such as Volvo, Ikea, Scania, ABB and Spotify. Skåne region is known for the number of entrepreneurs and start-ups that are developing their own ideas and putting them on the market. OMotion is one of those companies. The start-up had previous university students that develop their Master Theses within the company, so the university had information about possible Master Thesis projects to be developed with the company. The selection process was quick as the CEO of the company and the author had a few meetings and, shortly after, the contract was signed by both parties. The project was related to the field of expertise but also posed a challenge as there were some topics which would be needed to learn deeper. It would be the continuation of another two Master Theses developed one year before by students from Lund University, related to the development of a safety system to improve the driving performance of the vehicle. That facilitated the search for supervisors as the ones that supervised the previous Master Theses quickly were enrolled in the project. The company explained that all the equipment and tools required to perform the Master Thesis would be available. The Master Thesis is a research project that requires fieldwork to acquire the data needed.

### 3.2 Process

An empirical field investigation was carried out with the aim of improving the safety of the vehicle during driving through the development of the TCS. During the development of the work, there have been many issues and challenges that are addressed in this chapter. The Master Thesis follows a scientific-quantitative methodology meaning that there are issues encountered in the design and there are other issues encountered in the implementation of the design. As mentioned before, OMotion wants to develop its own customized TCS. This is the main focus of the Master Thesis. Using the controllers developed by the previous students as a basis, the aim

of the Master Thesis is to integrate them together, implement them in the vehicle and test it on the real vehicle to evaluate the performance, as the controllers have been tested separately previously. The controllers have previously been designed using multiple control strategies and then tested in the vehicle to choose the most favourable strategy among the previously designed and it is assumed that the control strategy chosen was the most adequate, so no further research was done on that topic and the control strategy for each control will not be changed. Along the lines of the second objective, mentioned in Section 1.1, before the work began, the vehicle had procedures to acquire data for OMotion that were done manually or in a non-optimal way. The aim was to find procedures or algorithms that process the data using automated approaches to obtain more precise and realistic values. One of these procedures is the calculation of the wheel's angle values. These values are important information that has a valuable use for OMotion. Another one of these procedures is the conversion of the current of the motor to torque. The reason why both of these data are relevant for the work carried out is explained in Chapter 4 and Section 5.6. The vehicle has seen some changes, so there needs to be tuning for some parameters and devices that are part of the vehicle. Specifically the gyroscope and accelerometer device and the cornering and longitudinal stiffness parameters. The gyroscope provides information about the yaw rate of the vehicle while the accelerometer provides information about the accelerations of the vehicle along its three axes. The cornering and longitudinal stiffness parameters have a strong influence on the wheels behaviours and having an accurate value of them will help to have a better understanding of the vehicle's behaviour while driving. During the development of the work, it was seen that the ABS system also needed to be tuned again. A final objective was set., related to the values of the control parameters of the traction control, developed by [Nilsson and Sandstedt, 2021]. The parameters for this control are difficult to tune and online adaptation is therefore of interest. A solution for the problem could be to add real-time identification and parameter estimation or an adaptation of the parameters of the controller, for example, using strategies such as gain scheduling. All of the steps mentioned above are meant to achieve one thing, to investigate if a correctly tuned TCS improves the safety of the vehicle while driving. To confirm this, the controllers need to be tuned with the correct parameters. Then, tests must be run to evaluate the performance of the vehicle with those parameters. Then, an evaluation of the performance is needed to investigate whether the behaviour of the vehicle is the one expected and if it indeed improves the safety of the vehicle.

The first step, agreed between OMotion and the author, was to start trying to develop the automatic approach to acquire the wheel's angle information. Previously, this data was calculated using only information of the steering wheel angle. Moving the steering wheel from one side to the other, a range of wheel's angles were measured manually with the vehicle remaining still. With this information, a curve was designed to fit the points as best as possible. This procedure is not accurate as the value of the wheel's angles is dynamically affected by more parameters

apart from the steering wheel angle, such as the vertical load and wheel alignment parameters, as OMotion mentioned and each wheel have different values for the same parameters. The suspension structure of OMotion2 will then need to be studied, as its dimensions, elements and wheel-alignment parameters are a key point to develop this procedure. OMotion provided the information regarding the suspension structure of OMotion2 and the values of the wheel alignment parameters. With this information, the procedure could start to be designed. The idea was to create a Matlab script that would provide information about the values of the wheel angle, the strut length and the camber angle for each wheel, providing as inputs the wheel alignment parameters, nominal lengths and relevant suspension structure points. It was done this way to be able to use the same script whenever the wheel alignment parameter change. The complete procedure is explained in Section 4. There were some issues that appeared throughout this process that made the development of this part more time consuming than it was expected. At the beginning, it was not clear what strategy to follow. Eventually, OMotion pointed towards an approach that turned out to work properly. Another issue was related to the computational power available. The procedure developed should be implemented in the vehicle using C/C++ programming language with a device that was limited by the hardware, meaning that the code could not have complex mathematical algorithms such as equation solvers and not many computational-power-consuming mathematical operation like square roots and divisions. The code needed to be as simple as possible and this posed a challenge. The Matlab script was coded like this as well, to be able to use it as a tool to see if the C code was well implemented. Once the Matlab code was developed, its functionality was checked. This was done by putting inputs whose output values were known. The code was modified correcting mistakes until the outputs matched the expected ones. Then, the C code was designed. This process was quicker than the design of the Matlab code as the latter was used as a reference. Once it was completely designed, the same inputs as before were used to see if the C code provided the outputs expected. Once this point was reached, the next step was to use this procedure while driving the vehicle to see if the output values (wheel's angles, strut length and camber angles) have reasonable values. This part was left for the last stages of the Master Thesis as more work was needed to be done before being able to drive the vehicle, like the tuning of the controllers.

The second step was to tune the devices mentioned. These were the gyroscope and the accelerometer. The gyroscope measures the angular velocity of its rotation in a reference frame along its three sensitivity axes in millidegrees per second while the accelerometer measures the acceleration in a reference frame along its three sensitivity axes in millimeter per second squared. The axes are relative to the device and do not match the vehicle's coordinate system. The reason these devices need to be tuned again is because the location of the device changed as well as its orientation. If the orientation is changed, the data need to be transformed into the coordinate system of the vehicle. The tuning procedure for these devices is explained in detail in Chapter 4. The information provided by these two devices is relevant so

the tuning is very important. The tuning consisted on running two tests. With the information provided by the test a rotation matrix will be made to transform the information from the devices to the proper coordinate system. Once this process was achieved, the new tuned parameters were implemented in the vehicle.

The next step was related to the conversion of current to torque. This conversion is important for OMotion because the torque is needed for the model as it is an input as well as for the control. If the conversion is inaccurate, the model would not be useful. Previously, the conversion was done using a factor. The value of this factor was estimated, as is seen in the work of [Nilsson and Sandstedt, 2021]. OMotion wanted to have a more precise and realistic conversion as it was suspected that it was not accurate to use a factor as the conversion could be affected by the velocity. So, a new procedure was developed to see what the actual relationship between the torque and the motor current was. To calculate this relationship, tests were run and the data obtained from these tests were transformed into torque using Matlab code. Then, the calculated torque and the motor current were contrasted together and its relationship studied. The new conversion procedure is explained in detail in Section 5.6. During the process, an issue arose. The current information could be extracted from two different points. One point was the current arriving to the inverter. The other point was the current exiting the inverter. Both currents should be the same, but there seemed to be an offset between them. A decision was made regarding which current information to use. Once the relationship between the current and the torque was obtained, which did indeed depend on the velocity, it was implemented in the vehicle, as well as the model.

The next step was the tuning of the model and its parameters. As the dimensions of the vehicle had changed, those changes needed to be updated in the model. As mentioned before, the model consists of mathematical representations that together can be used to simulate the behaviour of the vehicle. There are certain mathematical representations that have coefficients in their equations whose values are also affected by the dimensions of the vehicle, so they needed to be updated. There are also coefficients that are very relevant to have a good representation of the reality that previously were not set to an accurate value. These parameters are the cornering stiffness and the longitudinal stiffness. Previously, these values were estimated and modified until the model followed the real system, and the values that were used were outside of the normal range, so they were not accurate. Research was done to have a better understanding of the impact of these parameters in the model and more suitable values for the parameters were found. Once the parameters were updated, the integration of the controllers in the model was carried out. The traction control was already implemented in the model but the slip control was not. The integration of both controllers needed to be thought through and once the integration procedure was decided, simulations were run to test the behaviour of the integrated controllers. When the simulations were done, the model needed to be validated to see if it indeed represented the real system. Real data were needed to check this, so test needed to be run to gather data for the validation of the model, to see if the output of the model

and the output of the vehicle were the same, when the inputs for both of them were the same. When the tests were about to be done, it was realized that the ABS system also needed tuning as that is used to estimate the vehicle's velocity. The vehicle's velocity can be extracted using the ABS device output, if it is properly transformed. The outputs of the ABS are numbers that are transformed into speed values when they are multiplied by a factor. Previously, this factor was not accurate as it was estimated and then modified until reasonable values were obtained. Tests need to be run to acquire the new factor. The process of calculation of this factor is explained in detail in Section 5.2. During this process, an issue was encountered. The tests that were done turn out to be very sensitive, meaning that the factor that was obtained when the test was repeated a couple of time was not exactly same each time. An average value of the factors was used as the final result.

Once the ABS was tuned, test were run to acquire the data. During the process of validating the model, issues appeared as it was seen that the representation did not follow the same behaviour as the real system. After spending a period of time trying to figure out the reason why the model was not working, acquiring real data from the vehicle and inputting it on the model to check the outputs, the project moved to a different topic because of time constraints.

Once the devices were tuned, experiments with the real vehicle could be done. The first experiments that wanted to be carried out were the ones related to the calculation of the wheel's angles. To develop this experiment, a device to measure the real-time value of the steering wheel need to be introduce in the vehicle, with its corresponding tuning. When the device was tuned, the experiments began. They consisted of saving relevant data while making the vehicle take a turn. Two types of experiments were carried out. One for right turns and one for left turns. The implementation designed for the development is further explained in Chapter 9, while the analysis of the results obtained is further explained in Chapter 10.

At this point, more experiments using the vehicle could not be done because of time constraints.

### 3.3 Resources and Tools

The resources and tools needed for the development of the Master's Thesis are plenty. The software that is going to be used is essentially Matlab and Simulink [MathWorks, 2022] for simulation purposes and Microchip Studio for AVR [Microchip, 2022] as is the program used for the ECU. Matlab and Simulink are programming platforms that provide mathematical tools to design and analyse systems and use C/C++ and Matlab programming code. Microchip Studio is a program used to write and debug AVR applications and uses C/C++ programming languages. Other programs are used to acquire information while driving, such as Putty [Simon Tatham, 2022], which is a computer applications that emulates a terminal. Microsoft Office Excel 2020 and Matlab are used for the storage and treatment of

data collected in the fieldwork. In addition, experiments are going to be done to test if the work done is correct or incorrect. In those cases, the company will provide OMotion2 to acquire data while driving the vehicle. To have a better understanding of the suspension elements of OMotion2, AutoCAD [Autodesk, 2022] was used to analyse the elements one by one as well as all together.



# 4

## Front Wheel Alignment

In this chapter, the procedure developed to obtain the wheel's angles is explained using a mathematical approach. The steering ratio is the ratio between the steering wheel angle and the wheel angle. When the steering angle is equal to 1, it means that both angles are the same, whereas when it's different from 1, it means that other dynamics are causing the wheel angle to be different from the steering angle. This is the case with OMotion2. It is key to be able to have real-time data from the wheel's angle to design a precise control and to have an accurate model to perform accurate simulations. As mentioned before, the value of the wheel's angle is affected not only by the steering wheel angle, but also by the toe angle, the vertical load, and the dynamic camber angle. The caster angle also affects the wheel's angles value as the camber angle is impacted by the value of the caster. As the values change dynamically, two scenarios needed to be studied. The steady-state, where all the parameters have their nominal value, and the dynamic state, where the parameters change while driving. The nominal state needs to be studied since some parts of the front wheel structure will have different dimensions compared to the previous Master Theses. For example, to change the value of the camber angle, the length of an element of the structure needs to be physically modified. The same happens for the rest of the parameters. So, logically, the steady-state needs to be studied at least once, when the wheel-alignment parameters are set. The difference between the steady-state and the dynamic scenario is that the forces that act on the vehicle are constant for the steady state while the forces acting on the vehicle change dynamically while driving, in the other scenario.

### **Steady-State**

To aim of the steady-state investigation is to calculate the dimensions of the elements of the front wheel structure that change depending on the value of the ground clearance, the camber, caster and toe angle, automatically, instead of measuring them manually. The objective is to design an algorithm with those parameters as inputs and the dimensions of the relevant parts as outputs. This algorithm only needs to be run one time, after the wheel alignment of the vehicle has been done, as the

nominal value of the parameters will not change dynamically. The algorithm that was built works as follows: With the help of the program SolidWorks, specific coordinates for relevant points of the structure were obtained. The coordinate system is located in the vehicle as Figure 4.1 shows. The coordinate system is fixed at the vehicle, meaning that the axes are not fixed in space but in the vehicle. This means that certain points of the vehicle are always going to have the same coordinates, for example, points that belong to the metal structure of the vehicle. This is extremely useful, as the points will be the same in the steady-state as well as dynamically.

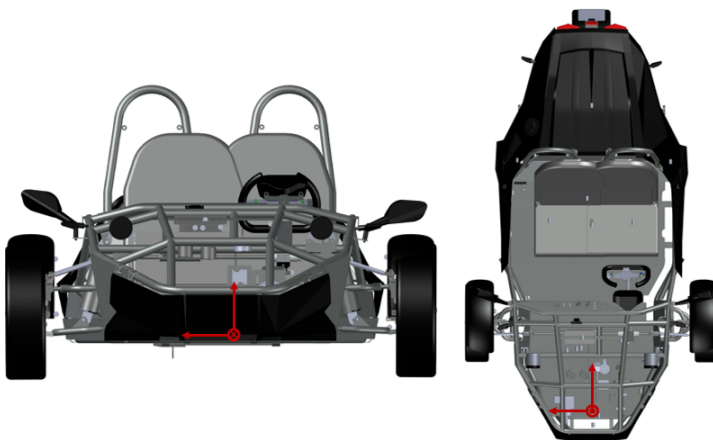


**Figure 4.1** Coordinates systems for front wheel suspension

With the coordinates obtained with SolidWorks and with wheel-alignment parameters, vectors were obtained to be able to move from one point to another. This way, if the lengths of the elements of the front wheel suspension system are modified (coordinates change), the vector will adapt to that variation as it will use the new coordinates. The algorithm used the magnitude and direction of the vectors obtained, 3D geometry and 3D trigonometry. Figure 4.2 shows a 2D plane with a few vectors that were used. A point needs to be made regarding the vectors. There were times when the vectors could be projected to a 2D plane, while there were others that needed to be studied in 3D, making the procedure more complex. Another point needs to be made regarding the coding complexity of the procedure. Even though the procedure was designed with Matlab, it needed to be implemented in the vehicle, that works with C code. This implementation demanded simple code and simple functions, so the Matlab code was designed to be simple and straightforward as well. The aim was that Matlab code and the C code were as similar as possible, so that the Matlab code could be used to check whether the calculations in C were correctly made.

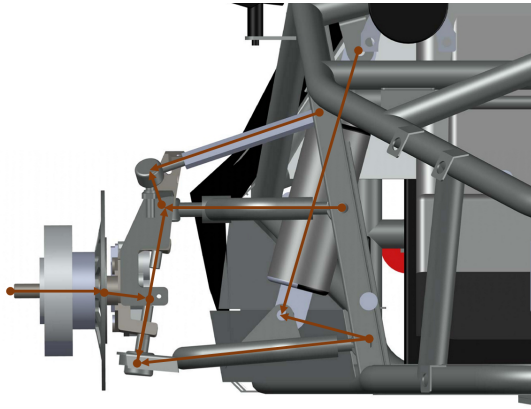


**Figure 4.2** Vector distribution for steady-state front wheel suspension

The disclosure of the complete procedure is not available as it is confidential information of OMotion, but it consists of calculating vectors between points of the suspension structure whose magnitudes will not change dynamically as it is physical impossible. This information was necessary for the dynamic-state module.

To summarise, the inputs that the steady-state computations required were the nominal values of the wheel alignment parameters and the coordinates of relevant points. The output of the steady-state computations were specific dimensions, angles and nominal forces acting on a specific element.

## Dynamic-State

Once the lengths of the elements of the front wheel suspension system are defined, the dynamic state can be calculated. The data that we are interested in that change while driving are the load on the strut and the steering wheel angle. The steering wheel angle is measured using a potentiometer. The value of the potentiometer needed to be tuned so that it provided a value of 0 when the steering wheel is pointing straight. The tuning of the device is explained in Section 5.3. The information of the strut load is calculated using the load on the tyre. The load of the tyre calculations are explained in Section 4 of this chapter. The load of the tyre is transferred to the strut. The vertical force is projected along the strut direction, as Figure 4.3 shows. To transfer the load, an iterative process is needed because depending on the force of the strut, the strut inclination and a point used in the middle of the calculations moves.

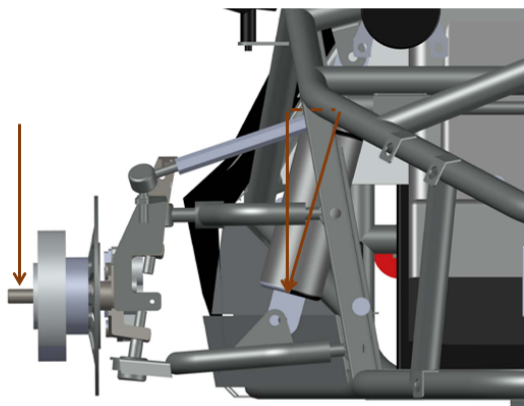


**Figure 4.3** Strut force from vertical tyre force

With the information of the force acting on the strut, the length of it can be obtained. With that length, relevant points can be calculated using the advantage of having the coordinate systems relative to the vehicle. Once these points are calculated using the information provided from the static calculations plus 3D trigonometry and vectors, the remaining relevant points are obtained. As mentioned before, some of the calculations were projected to a 2D plane, while there were others that need to be studied in 3D, making the procedure more complex. In addition, the coding complexity was reduced to the bare minimum so that the C-code was as simple as possible. A second degree equation solver function was developed to find the intersection of two vectors in space. As this procedure was used multiple times, a function was developed to optimize the code.

The disclosure of the complete procedure is not available as it is confidential information of OMotion, but it consists of using the magnitudes of the vectors computed in the steady-steady algorithm to obtain the dynamic values of the remaining suspension structure until the wheel angle can be obtained.

To summarise, the inputs that the dynamic-state required were the vertical load, the steering wheel angle and relevant dimensions of the suspension structure. The outputs of the dynamic-state are the wheel's angles, the strut lengths and the camber angles.

## Vertical Load

To calculate the vertical load, the Equation (4.1) [Lateral and Longitudinal Load Transfers 2022] was used. This equation is the combination of longitudinal and lateral load transfer and is given by

$$F_z = mgc - g \left( \frac{hma_x}{L} \right) \left( 0.5 \pm \frac{a_y h}{l_w} \right) \quad (4.1)$$

where  $m$  is the vehicle's weight plus the driver's weight,  $g$  is gravity,  $c$  is the percentage of the total force in a steady-state scenario that the front wheels take,  $h$  is the height of the COG,  $a_x$  and  $a_y$  are the acceleration of the vehicle along the x-axis and y-axis measured in N,  $L$  is the wheel base and  $l_w$  is the track width. The  $c$  value is calculated in the steady-state state using Newton's law and the equilibrium of forces.

When turning, the vehicle's load will be transferred from the inner wheels to the outer wheels and when accelerating or braking, the load will be transferred to the rear or the front wheels, respectively. The vehicle has three wheels, two in the front and one in the back and, as the distance to the COG from the rear wheel and the front wheels is not the same, the load on the front and the back wheels in the steady-state scenario are not the same. Equation (4.1) is a combination of lateral and longitudinal load transfer. Lateral load transfer happens when turning. The outer wheels take more force than the inner wheels. The longitudinal load transfer happens when accelerating or braking. The rear wheels take more force when accelerating, while the front wheels take more load when braking. The first term of the equation is the steady-state vertical load the front wheels have. It is the same for both wheels and it is measured in N. The second term is the longitudinal load transfer measured in N. The third term is the lateral load transfer measured in percentage. Depending on the direction that the vehicle is turning, the vertical load on a wheel should increase or decrease. Equation (4.1) can only be used when the accelerations of the vehicle are known. This is the case of the vehicle, as the information can be obtained by the accelerometer.

## Wheel angle

A point needs to be made regarding the sign convention for the wheel's angles. The calculations were made setting positive values for both wheels when the axis of the wheel is pointing to the right with respect to the z-axis of the vehicle, and vice versa, as Figure 4.4 shows. Another point needs to be made related to values. The wheel's will not have the same angle when turning because of the Ackerman steering geometry [Rajamani, 2012b]. As each wheel has a different curvature radius, the inner wheel needs to be steered with larger angles than the outer wheel, to avoid sliding.

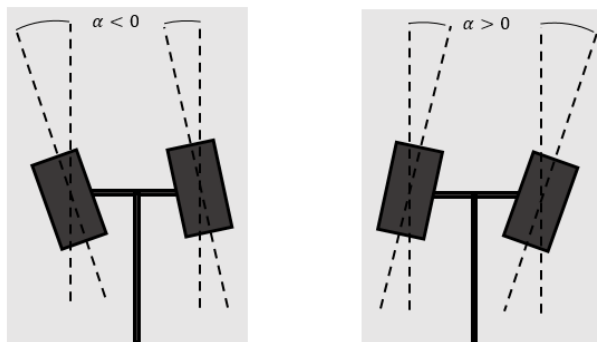


**Figure 4.4** Wheel angle sign convention

# 5

## Device and Model Parameters Tuning

In this chapter, the tuning of the devices mentioned in Section 3.2 is explained in detail. The devices that were tuned during the Master Thesis were the gyroscope and the accelerometer, the ABS and the steering wheel sensor. Moreover, as mentioned in Section 3.2, some parameters needed to be set to more reasonable values to have more accuracy in the model, such as the cornering and longitudinal stiffness and the dimensions of the vehicle. And lastly, the new conversion of current to torque mentioned in Section 3.2 is explained in detail as well.

### 5.1 Gyroscope and Accelerometer

The gyroscope is a device that measures the angular velocity of its rotation in a reference frame along its three sensitivity axes. The axes of the gyroscope do not match the axes of the OMotion2 vehicle, because the gyroscope is located at the front of the car in a plane that is not parallel to the XY, XZ or YZ plane, as Figure 5.1 shows. The accelerometer suffers from the same consequence as it is located at the same point with the same inclination as the gyroscope. The raw values that both devices provided are not in the desired system of coordinates. The data will need to be rotated with a rotation matrix so that the information is obtained in the correct coordinate system, as shown below:

$$\begin{pmatrix} \dot{x} \\ \dot{y} \\ \dot{z} \end{pmatrix} = R \begin{pmatrix} \dot{x}_m \\ \dot{y}_m \\ \dot{z}_m \end{pmatrix} \quad (5.1)$$

$$\begin{pmatrix} \dot{\Theta} \\ \dot{\Phi} \\ \dot{\Psi} \end{pmatrix} = R \begin{pmatrix} \dot{\Theta}_m \\ \dot{\Phi}_m \\ \dot{\Psi}_m \end{pmatrix} \quad (5.2)$$



**Figure 5.1** Displacement between gyroscope and accelerometer coordinate system

where  $\ddot{x}$ ,  $\ddot{y}$  and  $\ddot{z}$  are the acceleration along the x, y and z axis of the vehicle.  $\ddot{x}_m$ ,  $\ddot{y}_m$  and  $\ddot{z}_m$  are the acceleration along the x, y and z axis of the accelerometer.  $\Theta$ ,  $\Phi$  and  $\Psi$  are the vehicle's pitch, roll and yaw accelerations respectively.  $\Theta_m$ ,  $\Phi_m$  and  $\Psi_m$  are the gyroscope's pitch, roll and yaw acceleration respectively.  $R$  represents the rotation matrix.

To calculate the parameters of the rotation matrix, two tests were run. The first test consists of acquiring measurements from the gyroscope and the accelerometer with the vehicle level on the ground. The measurements that were obtained are the accelerations and the angular velocity of the levelled vehicle. The second test consists of acquiring measurements from the accelerometer with the vehicle tilted to a certain angle. In this test, the data needed are only the accelerations. Once the elements of the rotation matrix are calculated, the measurement is multiplied by them to be used in the simulation.

## 5.2 ABS

The ABS is a safety braking system. This device as implemented in the OMotion2 can also be used to calculate the speed of the vehicle with the output that it provides. The output needs to be turned into speed values, as they are just numbers without the tuning. The tuning consisted of making the ABS disc rotate around its axis and saving data to calculate a factor that, when multiplied by the output information of the ABS, provides a velocity. The data stored was the frequency of rotation of the ABS disc using an oscilloscope and saving the RPM information of the three sensors that are contained on the ABS device. Multiple tests were made, each of them changing the rotation speed of the ABS disc.

A point needs to be made about this tuning. The device has high sensibility, meaning that, under the same conditions (same rotation speed), the factor calculated was similar but not the same. For each rotation speed, multiple factors were calculated and then the average value was computed. Once the tests were run for



different rotation speeds, the factor was computed as the average of them

$$\chi = \sum_{i=1}^n \frac{\chi_i}{n} \quad (5.3)$$

where  $\chi$  is the final factor,  $\chi_i$  is the factor of each velocity and  $n$  is the number of tests performed.

### 5.3 Steering Wheel Sensor

The steering wheel angle is obtained using a potentiometer. The potentiometer is a device that has a variable resistance. The raw output of the sensor needs to be transformed into degree angles. The aim was to have a zero angle when the steering wheel is looking forward, and negative or positive angles when the steering is rotated. The sensor is really sensitive, so it was complicated to have a value of zero when the vehicle was driving straight. OMotion2 has the code for the tuning procedure already in the vehicle, so the tuning was done without any other issues.

The sensor provided a negative value when the steering was made to the right and a positive value when the steering was made to the left. The tuning was done after the coding and the implementation. It was assumed that the sensor would provide positive values when steering to the right and vice versa. As this was not the case, a negative sign was added in the C code when the information of the sensor is read.

The calculations were made before knowing this issue and they were designed the other way around: positive values when steering to the right and vice versa. So, when reading the data from the sensor, a negative sign is added for computational purposes.

### 5.4 Cornering and Longitudinal Stiffness

The cornering stiffness is one of the most important tyre parameters regarding the stability systems of the vehicle. It is the negative slope of the curve between the lateral force acting on the tyre and the tyre's slip angle. The accuracy of this parameter will affect the accuracy of the simulation. Its value depends on many other parameters, such as size, type, pressure, road surface and constitution of the tyres and the load, among others. So to speak, the value of this parameter is not constant. The previous Master Thesis [Nilsson and Sandstedt, 2021] used a constant value for this parameter. In this thesis, as the load has a strong influence on the cornering stiffness value, another approach was studied. The cornering stiffness value can be calculated as a percentage of the vertical load acting on the tyre. Normally, this percentage ranges between 8% and 18% [Gillespie, 1992]. The value will then change

dynamically. The longitudinal stiffness is another key parameter regarding the stability systems of the vehicle. It is the slope of the curve between the longitudinal force acting on the tyre and the tyre's slip ratio. As the previous parameter, its value is affected by many other parameters and it is not constant. It is strongly related to the cornering stiffness value. The previous Master Thesis [Nilsson and Sandstedt, 2021] used a constant value for this parameter. In this thesis, as the cornering stiffness has a strong influence on the longitudinal stiffness value, another approach was studied. The longitudinal stiffness value can be calculated by multiplying the cornering stiffness of the tyre by a factor. The longitudinal stiffness is normally 50% larger than the cornering stiffness [Pacejka, 2012]. The value of this parameter will also change dynamically, as the cornering stiffness is influenced by the vertical load.

Each wheel has its own cornering stiffness and longitudinal stiffness. But, as both wheels are the same, it was assumed that the values for both wheels will be the same. The cornering and longitudinal stiffness are implemented in the model. The real value of the parameters is not available as the manufacturer of the tyre did not provide it and also because it depends on the road surface. These coefficients are important for modelling purposes as they are part of the tyre model used for this project. The implementation of these parameters is explained in Chapter 6.

## **5.5 Dimensions of the Vehicle**

The dimensions of the vehicle have changed and so have the parameters that are affected by those dimensions, such as the position of the COG and the wheels' inertia, among other things. In addition, the weight of the vehicle has changed, and it is used to calculate the vertical load. The weight of the vehicle is known, but for the simulation to be accurate, the weight of the person driving also needs to be known. An assumption was made regarding this and extra weight was added.

## **5.6 Current to Torque Conversion**

As mentioned before, one of the inputs of the model is the torque the motor provides to the rear wheel. The torque is a quantity that is not provided by any device on the vehicle. On the other hand, the current is a measurement that is easily obtained through the controller area network (CAN) bus of the ECU. The current and the torque are related. The relationship between them is the topic of discussion in this section. The previous Master Thesis [Nilsson and Sandstedt, 2021] assumed it was a linear relationship. The torque was calculated by multiplying the current by a constant factor. In this section, a more precise calculation is developed as it is thought that the relationship is more complex. To study this relationship, an experiment was designed. In this test, the vehicle starts from rest and then the throttle is

pushed down completely until it reaches a certain velocity. While driving, the current and the motor speed are recorded. With the motor speed, the velocity in m/s is calculated and the acceleration too. With this information, the forces involved in the vehicle can be obtained. The torque provided to the rear wheel is the sum of the forces applied to that wheel multiplied by the radius of the wheel. Once the torque is calculated, it was contrasted with the current. The ratio between torque and current isn't constant and it depends on the velocity of the vehicle. The ratio was then contrasted with the velocity to investigate the relationship between the two. As Figure 5.2 shows, the ratio has different values for different velocities (yellow curve).

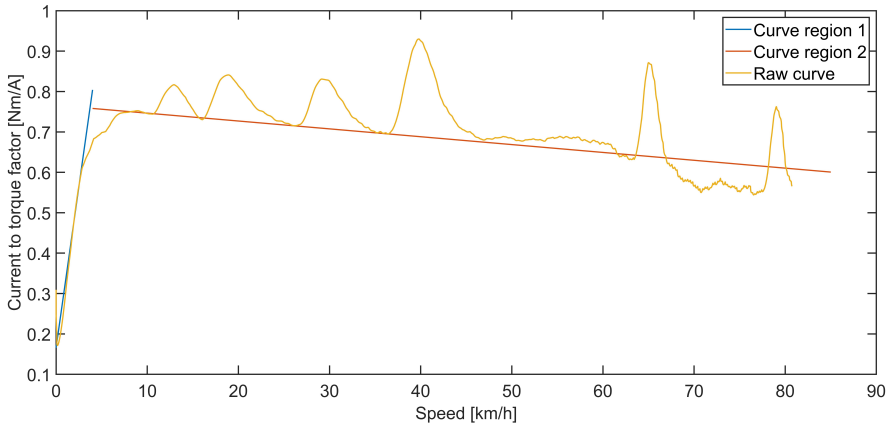


**Figure 5.2** Current-to-torque ratio vs velocity

Two different regions can be distinguished by looking at Figure 5.2. The first one, from 0 to 4 km/h and the second one from 4 km/h and above. In both regions, the relationship between the parameters can be seen to be as linear. A point needs to be made regarding the second region. The peaks of the ratio are not relevant in this case as the ratio is calculated using the motor speed provided by the vehicle and at some moments, the data acquisition is not as smooth as it should be. A curve for each region was fitted to represent the relationship as well as possible. The curves are defined by the following parameters: slope and y-intercept. Multiple tests were run but the curve's parameters from each test were slightly different. Therefore, the mean value of each parameter was calculated so that the curve could fit as well as possible for each test. Figure 5.2 shows the curves that are used in both regions. The torque is then calculated as follows:

$$\tau = f(V)I \quad (5.4)$$

$$f(V) = sV + q \quad (5.5)$$

where  $\tau$  is the torque,  $I$  is the current,  $V$  is the velocity,  $s$  is the slope of the curve,  $q$  is the y-intercept of the curve and  $f(V)$  represents the factor. This calculation is relevant both for the model and for the implementation of the slip control in the vehicle.

## 5.7 Filtering

On many occasions, the data that were provided by the vehicle was not smooth and presented a lot of peaks. In these cases, a low-pass filter was used to smooth the signal so that it could be better interpreted by the rest of the procedures. Figure 5.3 shows how the filter helps smoothing the input signals so that the peaks do not affect the calculations. The blue curve represents the raw data, while the red curve represents the filtered data.

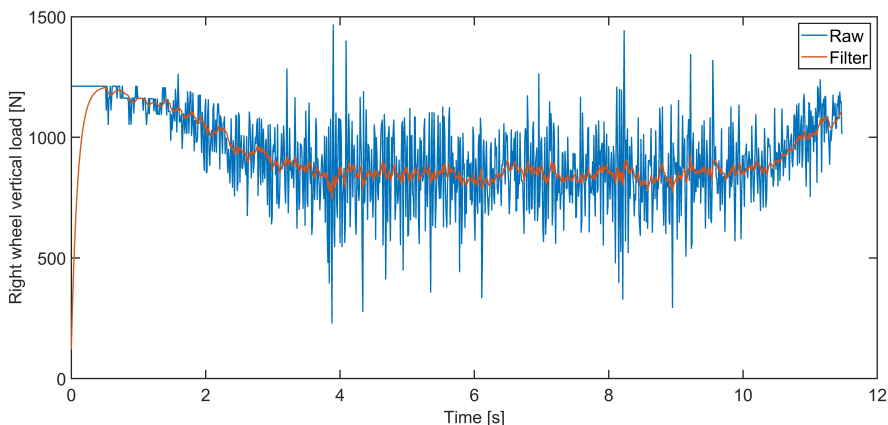


**Figure 5.3** Filtering of data used as input for computations

# 6

## Model

In this section, the model from literature that was used is explained, as well as the modifications that were made to improve it. The model consists of a group of mathematical representations organized by blocks. One block represents the wheel's dynamics, another block calculates the slip ratio for each wheel, another calculates the wheel's angles, another represents the tyre model, another represents the vehicle's dynamics and another one transforms the vehicle coordinates to the global coordinate system.

The inputs of the model are the initial speed, the initial yaw rate, the torque and the wheel's angle. All of these inputs can be obtained from the vehicle. The speed is provided by the ABS, the yaw rate is provided by the gyroscope, and the wheel's angle is provided by the procedure elaborated using the information of the vertical load and the steering wheel angle explained in Chapter 4 and, lastly, the torque is calculated converting the current of the motor that is provided by the CAN bus of the ECU with the conversion explained in Section 5.6. The outputs of the model are the speed of the vehicle along the X-axis and the Y-axis, as well as the yaw rate of the vehicle. The vehicle can also provide this information, using the ABS device and the gyroscope, as Figure 6.1 shows.  $I$  is the current of the motor,  $T_d$  is the torque converted,  $T_c$  is the controlled torque,  $T$  is the model input torque,  $w_0$  is the initial yaw rate,  $v_0$  is the initial speed,  $\delta_R$  and  $\delta_L$  are the right and left wheel angle,  $v$  is the traction control output variable,  $\sigma$  is the rear wheel slip ratio,  $\dot{x}$  and  $\dot{y}$  are the speed of the vehicle along the x-axis and the y-axis and lastly,  $\Psi$  is the yaw rate.

The current to torque block was introduced in the model. In the block, the conversion is implemented. As mentioned before, the conversion factor depends on the velocity of the vehicle. The integration of the slip control and the traction control is also introduced in the model. The slip control and the traction control strategy are explained in detail in Chapter 7. Previously, only the traction control was present in the model. The traction control was designed by [Nilsson and Sandstedt, 2021]. The inputs that the traction control need are the linear velocity of the vehicle, the yaw rate of the vehicle and the wheel's angles. The output of the traction control is a variable, which value could either be 0 or 1. This represents if the control is active or not. This variable is multiplied with the output of the slip control. The slip

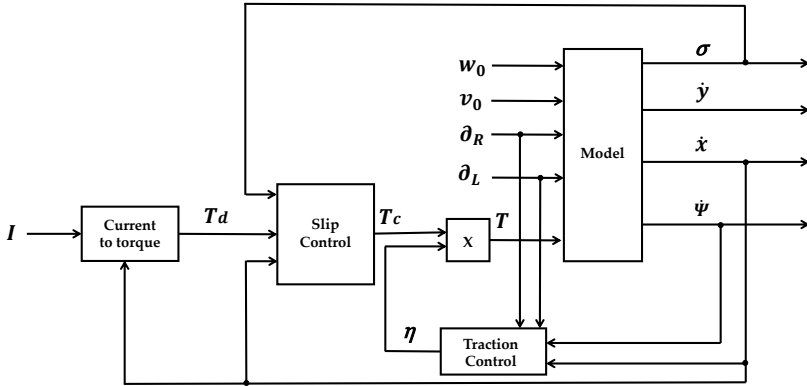


**Figure 6.1** Block diagram of the inputs and outputs of the model

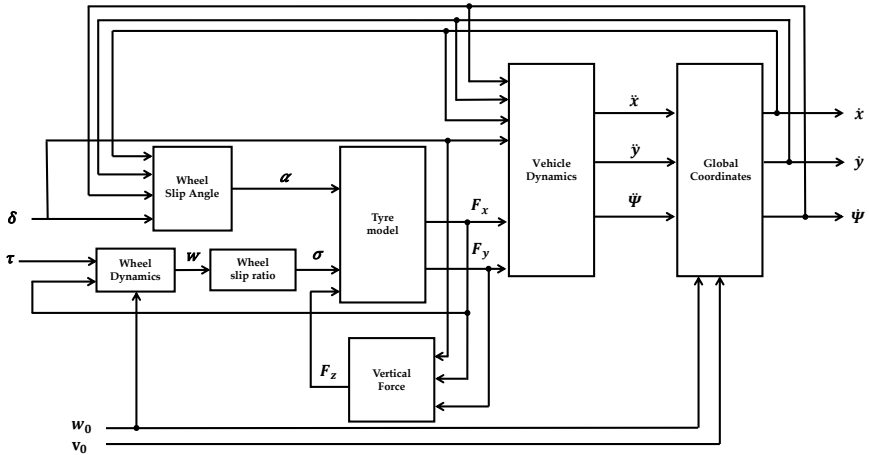
control was designed by [Karlin, 2021]. The input of the slip control is the motor torque, the linear velocity and the slip ratio while the output of the slip control is the control torque. The logical approach was to cascade both controllers meaning that the output of one control is the input of the other. When the grip between the tyres and the road is lost, the slip ratio becomes 1. The slip control helps maintain the slip ratio between a certain range, so it's wise to place the slip control before the traction control.

Figure 6.2 shows the block diagram of the model used.  $\tau$  is the model input torque,  $\delta$  represents the wheel's angles,  $w$  is the yaw rate,  $\sigma$  represents the wheel's slip ratios,  $\alpha$  represents the wheel's slip angles:  $F_x, F_y, F_z$  represent the forces along the x-axis, the y-axis and the z-axis.  $\ddot{x}$  and  $\ddot{y}$  are accelerations along the x-axis and the y-axis.  $\dot{\Psi}$  is the angular velocity of the vehicle.  $\dot{x}$  and  $\dot{y}$  are the speed of the vehicle along the x-axis and the y-axis and lastly,  $\Psi$  is the yaw rate of the vehicle.

The wheel's dynamics described in Section 2.4 are included in the respective block. Each wheel has its dynamic equations. As mentioned before, the torque is only applied at the rear wheel, as it is the driving wheel while the braking torque is applied at each wheel. This block did not undergo any changes in comparison with Nilsson and Sandstedt's model.

The wheel slip angles mentioned in Section 2.4 are included in the respective block. Each wheel has its slip angle. These calculations are required as they are needed inputs of the tyre model. This block did not undergo any changes in comparison with Nilsson and Sandstedt's model.

The wheel slip ratio explained in Section 2.4 is included in the respective block. Each wheel has its slip ratio. The slip ratios of the left front wheel and the right



**Figure 6.2** Block diagram of the model

front wheel are very similar as they are rolling wheels, meaning that the driving torque is not applied on the front axis, while the rear wheel is the wheel that will have a bigger slip ratio while accelerating. This block did not undergo any changes in comparison with Nilsson and Sandstedt's model. The tyre model calculates

The tyre model chosen by Nilsson and Sandstedt was the Dugoff's approach. This approach is explained in Section 2.4. The approach chosen was assumed to be the best suited for OMotion2, so no further research was done on that topic. The block takes the information of the wheel slip angle, the wheel slip ratio and the vertical force of each wheel to provide the lateral and longitudinal forces acting on each wheel. Small coding errors were found as the equations used in the model did not match the equations explained in Section 2.4. Also, the implementation of the cornering coefficients was changed. The new approach dictates that the normalised longitudinal and lateral slip ratios are calculated as follows:

$$\bar{\sigma} = \frac{\sigma CC_{\sigma} F_z}{\mu F_z (1 - \sigma)} \quad (6.1)$$

$$\bar{\alpha} = \frac{\tan(\alpha) CC_{\alpha} F_z}{\mu F_z (1 - \sigma)} \quad (6.2)$$

It can be seen that the vertical forces will not be affecting the value of the normalised longitudinal and lateral slip ratios, as the vertical force is present in the numerator and the denominator.

The procedure used to calculate the vertical load is using the equations of equilibrium of momentum. The dynamic forces that act on the vehicle are shown in

Figure 6.3 and Figure 6.4. The longitudinal and lateral forces of the front wheels are split into two terms, left and right because when turning, the forces acting on the wheels will not have the same value for both wheels. The equilibrium of mo-

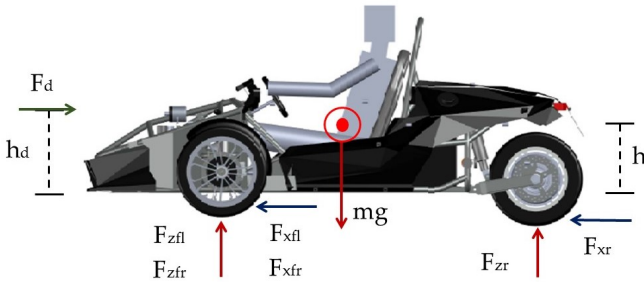


**Figure 6.3** Forces acting on the vehicle seen from the side

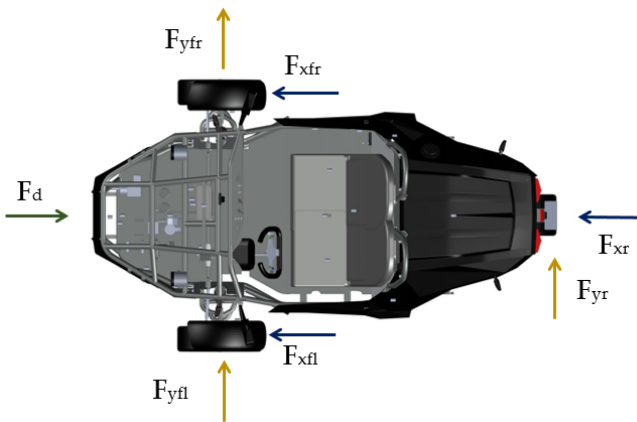


**Figure 6.4** Forces acting on the vehicle seen from above

mentum in each axis while turning is



$$0 = F_{zfl} \frac{l_w}{2} - F_{zfr} \frac{l_w}{2} + F_{xfl} \sin(\delta_{fl})h + F_{yfl} \cos(\delta_{fl})h + F_{yfr} \cos(\delta_{fr})h \\ + F_{xfr} \sin(\delta_{fr})h + F_{yr}h \quad (6.3)$$

$$0 = -F_{zfl}l_f - F_{zfr}l_f + F_{yfl} \sin(\delta_{fl})h - F_{xfl} \cos(\delta_{fl})h + F_{yfr} \sin(\delta_{fr})h \\ - F_{xfr} \cos(\delta_{fr})h - F_{xr}h - F_{zr}l_r - F_d h_d \quad (6.4)$$

$$I_z \ddot{\Psi} = F_{xfl} \sin(\delta_{fl})l_f + F_{xfr} \sin(\delta_{fr})l_f + F_{yfl} \cos(\delta_{fl})l_f + F_{yfr} \cos(\delta_{fr})l_f \\ - F_{xfl} \cos(\delta_{fl}) \frac{l_w}{2} + F_{xfr} \cos(\delta_{fr}) \frac{l_w}{2} + F_{yfl} \sin(\delta_{fl}) \frac{l_w}{2} - F_{yr}l_r \quad (6.5)$$

where  $F_{xfr}$ ,  $F_{xfl}$  and  $F_{xr}$  are the longitudinal forces on the front right wheel, front left wheel and rear wheel, respectively.  $F_{yfr}$ ,  $F_{yfl}$  and  $F_{yr}$  are the lateral forces on the front right wheel, front left wheel and rear wheel, respectively.  $F_{zfr}$ ,  $F_{zfl}$  and  $F_{zr}$  are the vertical forces on the front right wheel, front left wheel and rear wheel, respectively.  $F_d$  is the vehicle's air resistance.  $l_w$  is the distance between the front wheels' rotational axes,  $l_f$  is the distance from the COG to the front axle and  $l_r$  is the distance from COG to the rear axle.  $h$  is the height of the COG of the vehicle and  $h_d$  is the height of the air resistance force application point.  $\delta_{fl}$ ,  $\delta_{fr}$  and  $\delta_r$  are the angle of the front right wheel, the front left wheel and the rear wheel respectively.  $I_z$  is the vehicle's moment of inertia around z and  $\dot{\Psi}$  is the angular velocity of the vehicle.

The procedure to calculate the vehicle's dynamics is using the equations for the balances of forces. The balances of forces while turning are shown in Equation (6.6) for the X-axis, Equation (6.7) for the Y-axis and Equation (6.8) for the Z-axis:

$$m(\ddot{x} - \dot{\Psi}\dot{y}) = F_{xfl} \cos(\delta_{fl}) + F_{xfr} \cos(\delta_{fr}) + F_{fx} - F_{rx} - F_d - F_{yfl} \sin(\delta_{fl}) \\ - F_{yfr} \sin(\delta_{fr}) \quad (6.6)$$

$$m(\ddot{y} - \dot{\Psi}\dot{x}) = F_{yfl} \cos(\delta_{fl}) + F_{xfl} \sin(\delta_{fl}) + F_{yfr} \cos(\delta_{fr}) + F_{xfr} \sin(\delta_{fr}) \\ + F_{yr} \quad (6.7)$$

$$mg = F_{zfr} + F_{zfl} + F_{zr} \quad (6.8)$$

To obtain the velocities of the vehicle in the global coordinate system, Equations (6.9), (6.10) and (6.11) are used. These equations are included in the Global Coordinate block and are the following:

$$\Psi = \int \left[ \int \ddot{\Psi} dt + \dot{\Psi}_0 \right] dt \quad (6.9)$$

$$X = \int \left[ \int (\ddot{x} \cos(\Psi) - \ddot{y} \sin(\Psi)) dt + \dot{x}_0 \right] dt \quad (6.10)$$

$$Y = \int \int (\ddot{x} \sin(\Psi) + \ddot{y} \cos(\Psi)) dt dt \quad (6.11)$$

# 7

## Controllers

Traction control is a safety feature that vehicles have to assist to keep a grip between the road and the tyres of the vehicle when road conditions are dangerous or slippery. Slip control would help with this issue as well. Both controllers are key to having a safe vehicle performance. In this chapter, the logic around both controllers is explained. The study and research of the best control strategy for both controllers and the decision of which of the control strategies to implement in the vehicle was already done by [Nilsson and Sandstedt, 2021] and [Karlin, 2021]. In this Master Thesis, the control strategies implemented are the ones chosen by the previous theses. This Master Thesis does not focus on the study and research of the best control strategy, as that was developed previously. The controllers are explained here to have a better understanding of the integration that is needed. First, the control strategy for the slip control is explained, then the control strategy for the traction control and afterwards the interaction between them and the integration of both of them as one are discussed.

### 7.1 Slip Control

As mentioned before in Section 2.4, the slip ratio is a ratio used to measure the grip of the vehicle on the road. The slip control oversees the slip ratio. Under certain road conditions, the slip ratio should not be higher than a certain safety threshold value. When that value is exceeded, the control should act to force the slip ratio to the desired value. To force the slip ratio to a certain level, the torque needs to be controlled. As mentioned before, torque is not a directly measurable quantity. Instead, the current will be controlled and then converted to torque. This conversion is further explained in Section 5.6. A PI controller was the control strategy implemented by the previous theses as it was the one among many that performed the best [Karlin, 2021]. The block diagram used previously for this control is shown in Figure 7.1.

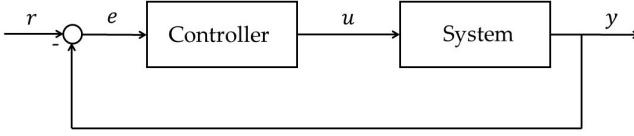


**Figure 7.1** Block diagram of the slip control

The manipulated variable of the control  $u$  is described as follows:

$$u = Ke(t) + \frac{K}{T_i} \int_0^T e(t)dt \quad (7.1)$$

where  $K$  is the proportional gain of the control and  $T_i$  is the integral time constant of the control. It is also common to use this parameter as an integral gain  $K_i = K/T_i$ . The error is the difference between the reference signal and the output signal of the control,  $e = r - y$ . In this case,  $r$  is the slip reference and  $y$  is the real-time slip ratio value. In this control, two situations need to be discussed: acceleration and braking. Two slip controllers will run at the same time. When the torque provided by the driver is positive, the slip control that will be activated, if the situation demands it, will be the acceleration slip control. On the other hand, if the torque provided by the driver is negative, the control that will be activated will be the braking slip control. Control logic from [Karlin, 2021] is used to choose between both controllers.

The acceleration control logic works as follows: the slip control should only be activated when the slip ratio exceeds the security threshold value. To avoid any unnecessary activation because of noisy signals, or the activation of the control with slow velocities, another two conditions are included: It should be activated when the slip ratio is bigger than the threshold value when the torque provided by the throttle of the vehicle is bigger than the torque calculated with the PI control and when the linear velocity of the vehicle is bigger than a certain value, as seen below:

$$\text{Control On if } (\sigma > \sigma_{th}^a) \& (T_d > T_c^a) \& (v > v_{th}) \quad (7.2)$$

To deactivate the control, the condition that should be satisfied is the following:

$$\text{Control Off if } (T_d < T_c^a) \quad (7.3)$$

For a braking situation, the control works as follows: the slip control should only be activated when the slip ratio exceeds the safety threshold value (this value is negative in this case) when the torque provided by the driver is lower than the torque provided by the PI controller and when the linear velocity of the vehicle is bigger than a certain value, as shown below:

$$\text{Control On if } (\sigma < \sigma_{th}^a) \& (T_d < T_c^a) \& (v > v_{th}) \quad (7.4)$$

To deactivate the control, the condition that should be satisfied is the following:

$$\text{Control Off if } (T_d < T_c^a) \quad (7.5)$$

Inside both controllers, a distinction is needed between dry and wet roads. This means that the proportional value will be different depending on the operating conditions. Once the control variable is obtained, it needs to be checked whether its value has exceeded a saturation value, as the signal's value needs to range between two limits. The value of the control parameters needs to be studied once again to tune them to achieve better performance. The tuning of the control is discussed in Section 7.4.

## 7.2 Traction Control

When a vehicle loses grip when turning, it means that the friction force exceeded the maximum friction force available. This causes the vehicle to start sliding because of the loss of grip and therefore the yaw rate increases. To cease the increase of the yaw rate, a torque must be applied to the vehicle to counteract the increase in the yaw rate. If the torque of the wheel is decreased, so will the angular velocity of the wheel, as Equation (2.9) shows. Then the wheel's angular velocity will decrease and go back to having a grip on the road, thus to a controlled situation again. The traction control oversees the torque applied to the rear wheel. Under a situation where the vehicle has a grip on the road, the torque applied to the wheel should come from the throttle, pushed by the driver. Under certain driving situations such as traction loss, the torque applied to the rear wheel cannot be set by the driver and needs to be controlled until the vehicle gains grip on the road again. When traction is lost, the value of the actual yaw rate of the vehicle and the expected value of the yaw rate will differ. The former is obtained from the gyroscope while the latter is calculated based on the linear velocity of the vehicle and the wheel angles. The difference between both of them will be known as the error of the traction control. The previous thesis calculated the desired yaw rate following the Equation (7.6) [Nilsson and Sandstedt, 2021]. This equation was developed by [Rajamani, 2012b] and is given by

$$\dot{\Psi}_{des} = \frac{\dot{x}}{R} = \frac{\dot{x}\delta_{ss}}{L + K_v\dot{x}^2} \quad (7.6)$$

where  $\delta_{ss}$  is the the steady state steering angle for driving in a curve of radius  $R$ ,  $L$  is the wheel base,  $\dot{x}$  is the velocity along the x-axis and  $K_v$  is the understeer gradient, that is given by [Rajamani, 2012b]:

$$K_v = \frac{l_r m}{2C_{\alpha f} L} - \frac{l_f m}{C_{\alpha r} L} \quad (7.7)$$

where  $l_f$  is the distance from the COG to the front axle and  $l_r$  is the distance from COG to the rear axle.  $m$  is the weight of the vehicle,  $L$  is the wheel base and  $C_{\alpha_f}$  and  $C_{\alpha_r}$  are the cornering stiffness coefficients of the front wheel and the rear wheel.

The error is calculated as

$$e = \begin{cases} |\dot{\Psi}| - |\dot{\Psi}_{des}|, & \text{if } \text{sign}(\dot{\Psi}) = \text{sign}(\dot{\Psi}_{des}) \\ |\dot{\Psi}| + |\dot{\Psi}_{des}|, & \text{if } \text{sign}(\dot{\Psi}) \neq \text{sign}(\dot{\Psi}_{des}) \end{cases} \quad (7.8)$$

If this error is lower than a certain threshold value, the control does not need to act and the torque stays uncontrolled. But if the error exceeds a certain threshold value, the torque is controlled until the error returns to the desired value. The value of that threshold is a topic that will be studied in Section 7.4. As mentioned before, torque is not a measurable quantity. Instead, the current will be controlled and then converted to torque. This is further explained in Section 5.6.

The control strategy from [Nilsson and Sandstedt, 2021] for the traction control is as follows: when a loss of grip happens while accelerating, the actual yaw rate increases with respect to the desired one. To return to a safe state, the torque must become zero so that it does not increase the wheel angular velocity. This can be seen in Equation (2.11). The same happens while braking. To put it in other words, when the control is on, the torque must be zero and when the control is off, the torque's value does not change. Following this line of thought, the previous thesis [Nilsson and Sandstedt, 2021] deemed it appropriate to use an on-off controller with hysteresis. When the error of the control is bigger than a certain threshold  $e_1$ , the traction control turns on. To make sure that the vehicle has gained grip again, the control would be turned off when the error is smaller than the threshold  $e_2$ , whose value is smaller than the previous one, as Figure 7.2 shows:

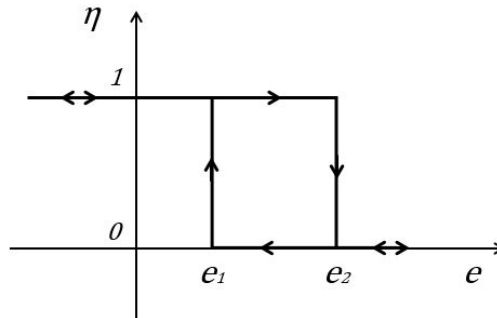


**Figure 7.2** Traction on-off control with hysteresis

where  $v$  is the output variable of the traction control,  $e_1$  is the lower threshold and  $e_2$  is the upper threshold. A point needs to be made about the value of the

error. Figure 7.2 shows that only positive values for the error are being taken into account. However there can be a situation where the error is negative, for example, when both yaw rates have the same values but the desired one is bigger, the error is negative. This situation is in fact a positive one, in terms of the control strategy, because it means that the vehicle's actual yaw rate is lower than the actual one. When this happens, the vehicle is suffering oversteer, while when the desired yaw rate is smaller than the actual yaw rate, it is known as understeer. The control is designed to stop the oversteer of the vehicle, not the understeer. So in this case, the situation when the error is negative is outside of the scope of the Master Thesis. The value of the output of the controller is feedback to be multiplied by the input torque as Figure 7.3 shows:

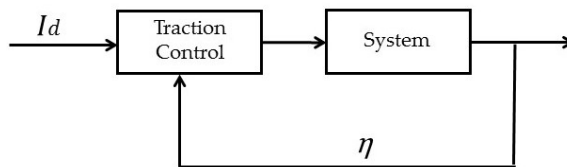


**Figure 7.3** Traction on-off control with hysteresis

where  $I_d$  is the current of the motor and  $v$  is the output variable of the traction control.

### 7.3 Integration

An integration of both controllers is needed to improve the vehicle's performance while driving. As seen before, the input of the slip control was the current of the motor, which is later on transformed into torque. The output of that control was the controlled torque. Meanwhile, the input of the traction control was the current of the motor, which was, later on, transformed to torque too. The output of that control is a value, either a 1 or a 0 that is then multiplied by the input torque to form a closed loop. The logical approach is to concatenate both controllers in a cascade structure. The output of one control is the input of the other. When the grip between the tyres and the road is lost, the slip ratio becomes 1. The slip control helps maintain the slip ratio between a certain range, so it is wise to place the slip control before the traction control. The block diagram of the integration of both controllers is shown below:

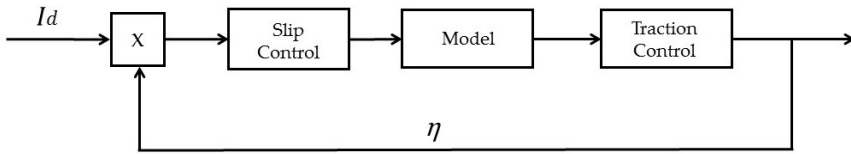


**Figure 7.4** Simple block diagram of the integration of the controllers

where  $I_d$  is the current of the motor and  $v$  is the output variable of the traction control. The current provided by the traction control will be fed to the motor of the vehicle, to provide the torque computed.

The parameters of the controllers, like the on-off thresholds, the slip ratio thresholds and such need to be studied again, because with the integration of both controllers, if the previous parameters were to be used, the performance of the vehicle will be different. This is further discussed in Section 7.4.

## 7.4 Tuning

### Slip Control

The slip control was chosen to be tuned first, as it is the first control to act. There are multiple parameters involved in the control: the PI control parameters and the slip ratio thresholds. These are constant parameters that are used to set the maximum and minimum value of the slip ratio. A distinction is needed between accelerating and braking. In the case of the former one, the threshold values will be positive while in the latter, the threshold values will be negative. Another distinction is required, in this case regarding the road conditions, whether the road is wet or dry. This applies as well to the PI parameters. Tuning is required for dry and wet asphalt and braking and accelerating.

The values of these parameters need to be studied to investigate what values are better fitted to the vehicle performance. Because of time constraints and model inaccuracies, the tuning of the control parameters could not be done. A couple of experiments were done to set new slip ratio thresholds. As it will be explained in Chapter 10, the thresholds that were experimented with were 0.1 and -0.15 for acceleration and braking, respectively, on gravel roads. Other values were not tested because of time constraints.

### Traction Control

The tuning of the On-Off traction control was not done because time constraints and model inaccuracies.

# 8

## Simulation

### 8.1 Integration of Controllers

To make certain that the integration of the controllers was adequate, simulations were carried out to evaluate the performances of the controllers under certain conditions. Table 8.1 summarises the behaviour expected of the controller. The slip control has to be active when the slip ratio is bigger than the threshold. The traction control has to be active when the actual yaw rate is bigger than the desired yaw rate. The control parameters that were used were the ones designed by [Nilsson and Sandstedt, 2021] and [Karlin, 2021]. The simulation aimed to investigate if the behaviour of the model matched the expectations.

**Table 8.1** Behaviour of controllers

|                  | Traction Control ON | Traction Control OFF               |
|------------------|---------------------|------------------------------------|
| Slip Control ON  | Input Torque = 0    | Input Torque = Slip Control Torque |
| Slip Control OFF | Input Torque = 0    | Input Torque = Driver Torque       |

A left turn was simulated. The inputs of the model were set. The initial yaw rate was set to zero, the initial velocity was set to 5km/h and the torque and the front wheels were set to simulate a left turn while accelerating the vehicle. The road conditions are set as for asphalt.

The first simulation that was carried out was to investigate the behaviour of the system when none of the controllers are turned on. The slip ratio threshold is set to 0.025 and the hysteresis values are set to 7 for the upper limit and 3 for the lower limit, as [Karlin, 2021] suggests in his work. During the simulation, extra torque is added to the input torque to see how the vehicle will react when the added torque is not big enough to turn both controllers on. Figure 8.1 shows the rear slip ratio. The effect of the added torque can be seen, but the value never reaches the 0.025 threshold, so the slip controller is not active. The slip starts with a zero value and quickly rises to 0.015. Figure 8.2 shows the input torque that the model receives. There are two curves plotted together. The blue curve is the controlled torque while



the black curve is the driver's torque. As the slip control is not active, the driver's torque and the controlled torque are the same. Figure 8.3 shows the yaw rate of the vehicle in black and the desired yaw rate in blue. The vehicle seems to be able to make the turn without any sliding situation. Figure 8.5 and Figure 8.4 show that none of the controllers were active during this simulation, as the slip control is equal to zero and the output of the traction control is 1.

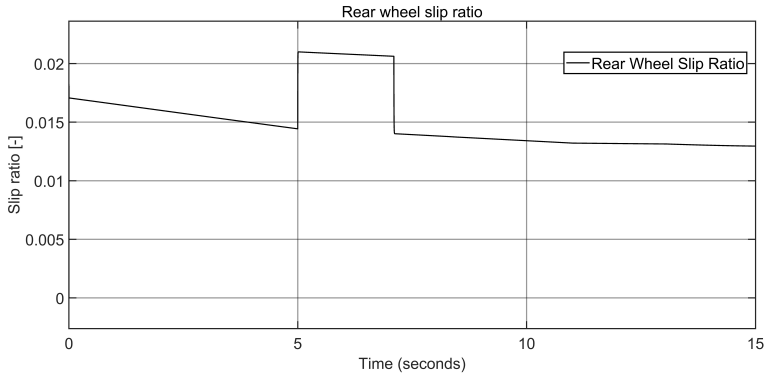


**Figure 8.1** Slip ratio with slip control off and traction control off

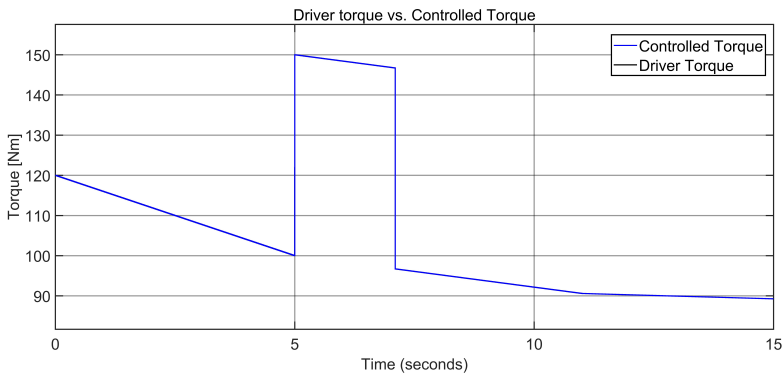


**Figure 8.2** Input torque with slip control off and traction control off

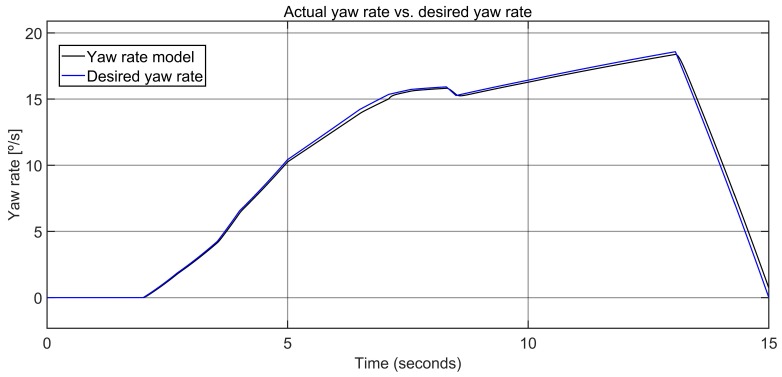


**Figure 8.3** Yaw rate with slip control off and traction control off

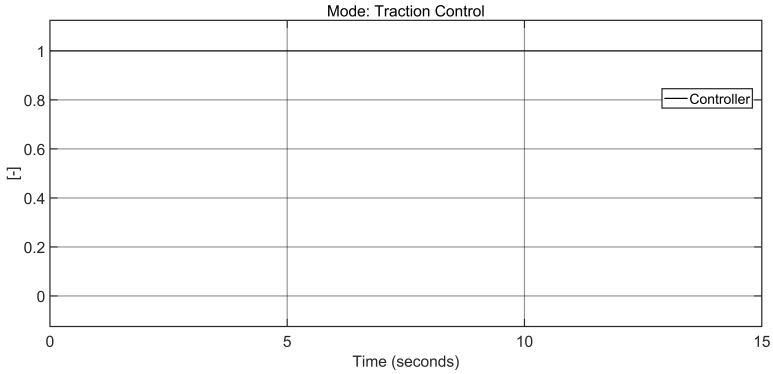


**Figure 8.4** Traction control mode with slip control off and traction control off

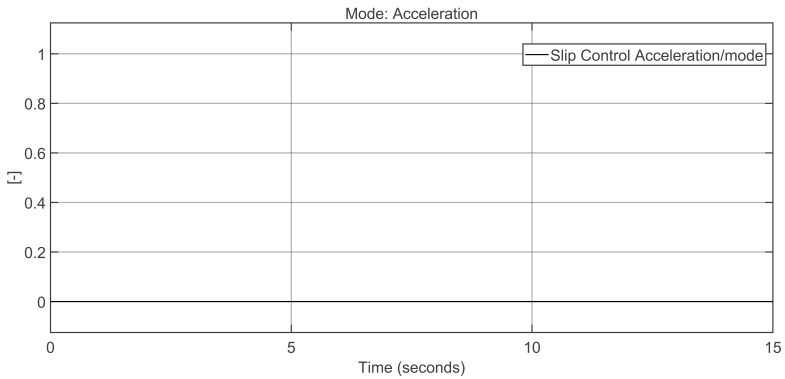


**Figure 8.5** Slip control mode with slip control off and traction control off

The second simulation that was carried out was to investigate if the slip control turns on when the slip ratio reaches a certain threshold. To achieve this, at a certain moment of the simulation, an extra torque was added to the input torque, bigger than in the previous simulation. The rear slip ratio calculated without the slip control active was higher than 0.02, so the threshold was set to 0.02 to see if it indeed turned on. Figure 8.6 shows how the rear wheel slip ratio, once it reaches the value of 0.02, decreases to smaller values. It happens at 5s, the same time as when the extra torque is added. Figure 8.7 shows how the slip control forces the controlled torque to smaller values than the driver's input. The blue curve is the controlled torque while the black curve is the driver's torque. The torque that is sent to the model is the blue curve, the controlled torque. Figure 8.8 shows the period the slip control stays on. The behaviour is the expected one. The slip turns on when the slip ratio is bigger than the desired and it turns off when the slip ratio is smaller than the threshold and when the controlled torque saturates at the driver torque. In this simulation, the traction control does not turn on, as in Figure 8.9, and it can also be seen in the input torque value as it does not have zero values for an extended period. With this simulation, the on-off behaviour of the slip control was tested.

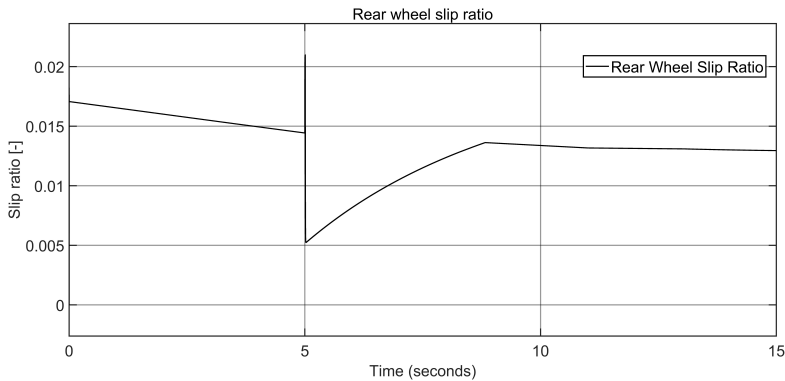


**Figure 8.6** Slip ratio with slip control on and traction control off

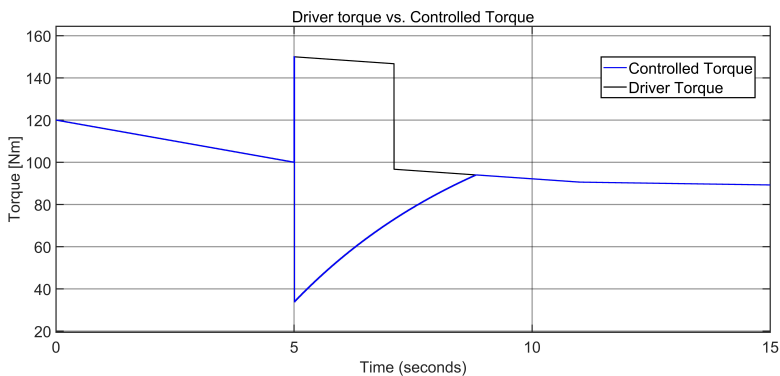


**Figure 8.7** Input torque with slip control on and traction control off

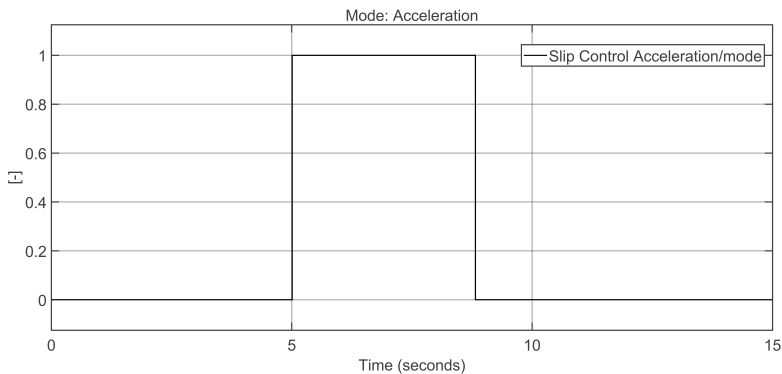


**Figure 8.8** Slip control mode with slip control on and traction control off

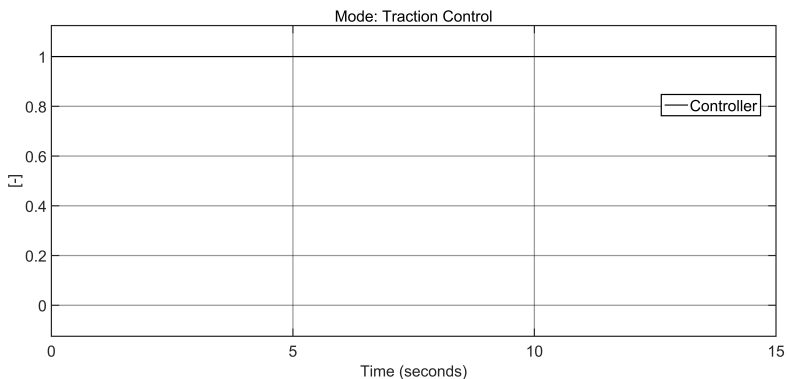


**Figure 8.9** Traction control mode with slip control on and traction control off

The third simulation that was carried out was to investigate if the traction control turns on when the vehicle's yaw rate is bigger than the desired yaw rate. To achieve this, the input torque will be bigger than the previous simulations as well as the wheel's angles, to simulate a sideways sliding situation. At a certain moment of the simulation, extra torque is added to the input torque, simulating that the driver has pushed the throttle down while taking a turn. The slip threshold will be bigger in this case because of the bigger torque and it was set to 0.1. The hysteresis values are set to 7 for the upper limit and 3 for the lower limit. These values were set following [Karlin, 2021] guidelines. Figure 8.10 shows the rear slip ratio. It can be seen that the value never reaches the threshold so the slip control is not active. Also, the effect of the traction control can be noticed in the rear wheel slip ratio, as it becomes zero when the control is on. Figure 8.11 shows the controlled torque, in blue and the driver's torque in black. The torque that is sent to the model is the blue curve, the controlled torque. As the slip control is not active, when the traction control is off, the torque becomes zero when the traction control turns on and it goes back to positive values when the traction control turns off. Figure 8.12 shows the period the traction control is on and when it is off. Figure 8.13 shows the effect that the traction control has on the vehicle's dynamics. As the torque becomes zero, the speed of the vehicle decreases until the traction control turns off and it starts to increase again. Lastly, Figure 8.14 shows the contrast between the actual yaw rate in black and the desired yaw rate in blue. When the difference between them reaches the upper limit, the traction control turns on until the difference between them reaches the lower limit, when the traction control turns off. The moment the traction control turns on and off can be noticed.

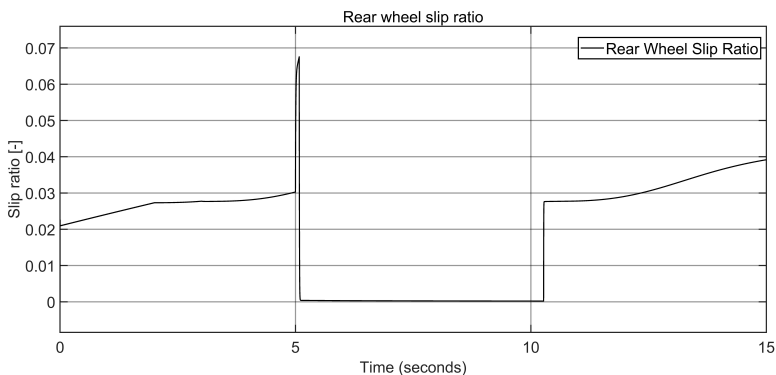


**Figure 8.10** Slip ratio with slip control on and traction control on

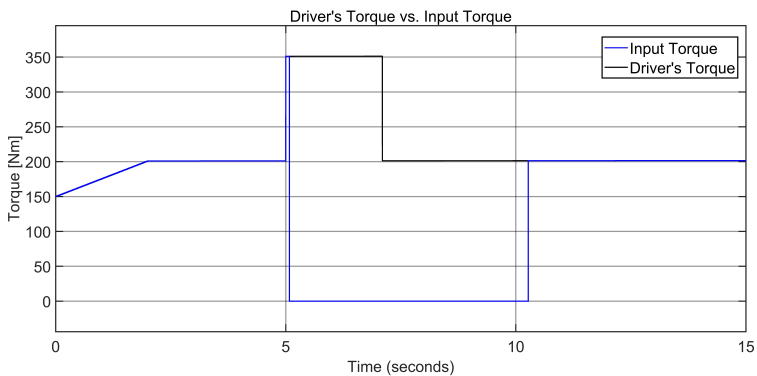


**Figure 8.11** Input torque with slip control off and traction control on

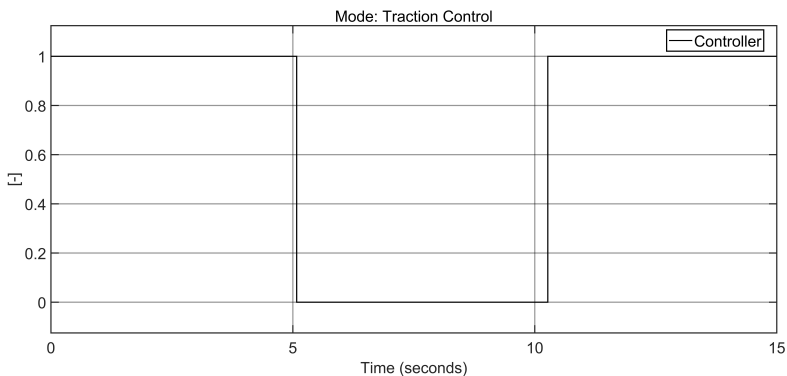


**Figure 8.12** Traction control mode with slip control on and traction control off

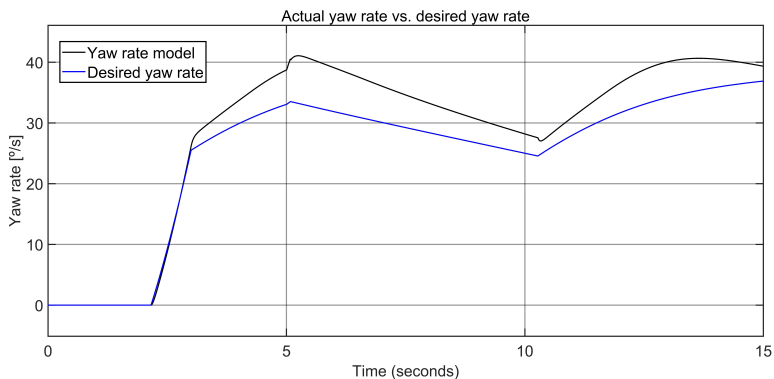


**Figure 8.14** Actual yaw rate and desired yaw rate with slip control off and traction control on

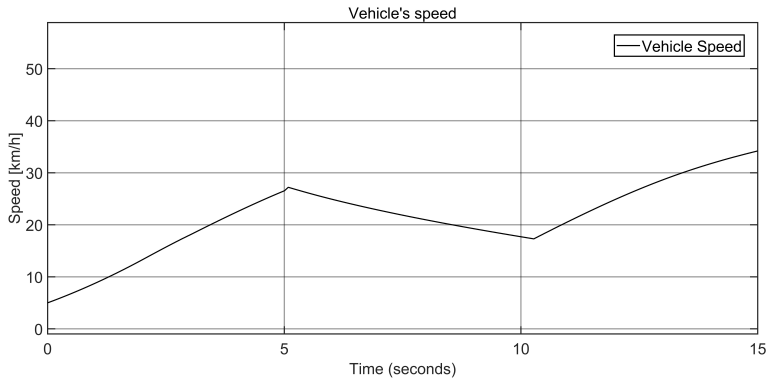


**Figure 8.13** Vehicle's speed with slip control off and traction control on

The last simulation that was carried out was to investigate how the controllers will behave when both of them are active. To achieve this, the input torque will be the same as in the previous simulations as well as the wheel's angles, but the slip ratio threshold will be lowered. At a certain moment of the simulation, extra torque is added to the input torque, simulating that the driver has pushed the throttle down while taking a turn. The slip threshold was set to 0.05 while the hysteresis values are set to 7 for the upper limit and 3 for the lower limit. Figure 8.15 shows the rear slip ratio. It can be seen that the slip is bigger than the threshold, so the slip control turns on and forces the slip ratio to move to lower values. From 5 s to 7 s, only the slip control is active and the traction control turns on 7 s. Figure 8.16 shows the input torque of the model in black and the driver's torque in blue. When the slip control turns on, the slip control forces the torque to lower levels to maintain the slip ratio below a certain level. When the traction control turns on, the slip control is overrun and the torque becomes zero until the traction control turns off. Figure 8.17 shows the actual yaw rate of the vehicle in black and the desired yaw rate in blue during the simulation. At 7 s, when the extra torque is added, the difference between the curves becomes greater than the upper limit and the traction control turns on. Both yaw rates become zero at the end as the cornering has ended. Figure 8.19 shows the period the slip control stays on. It can be seen that the slip control does not turn off over the simulated time period. If the simulation was longer, the controlled torque will saturate at the driver's torque and the slip control will turn off. Figure 8.18 shows the period the traction control stays on during the simulation.

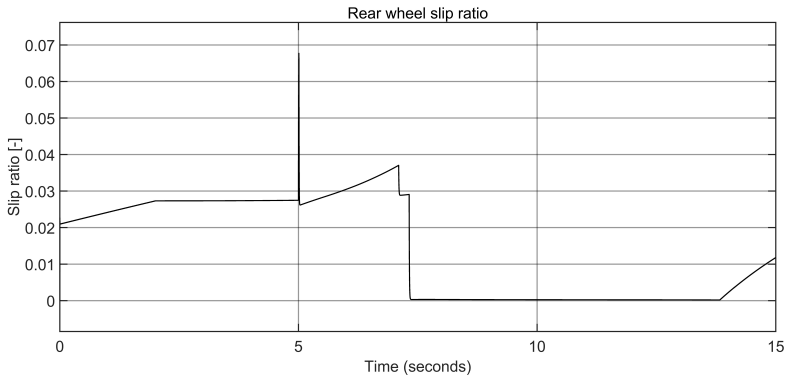


**Figure 8.15** Slip ratio with slip control on and traction control on

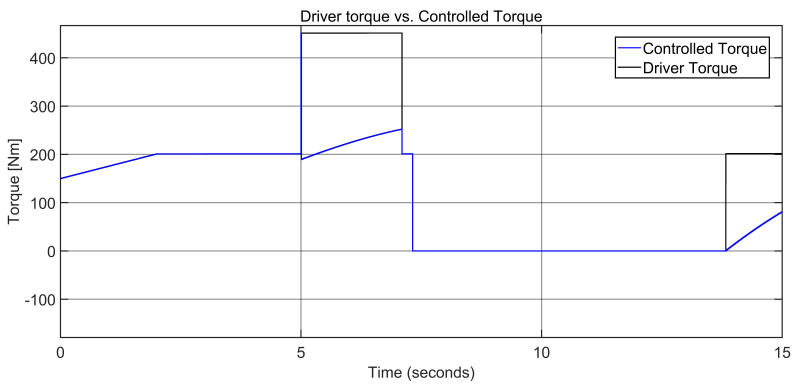


**Figure 8.16** Input torque with slip control on and traction control on



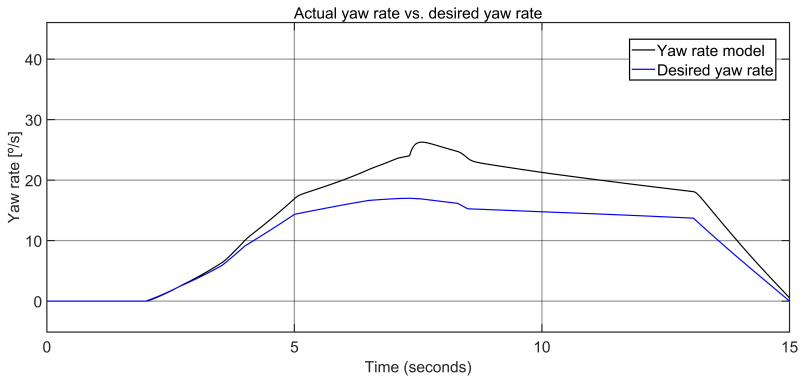


**Figure 8.17** Actual yaw rate and desired yaw rate with slip control on and traction control on

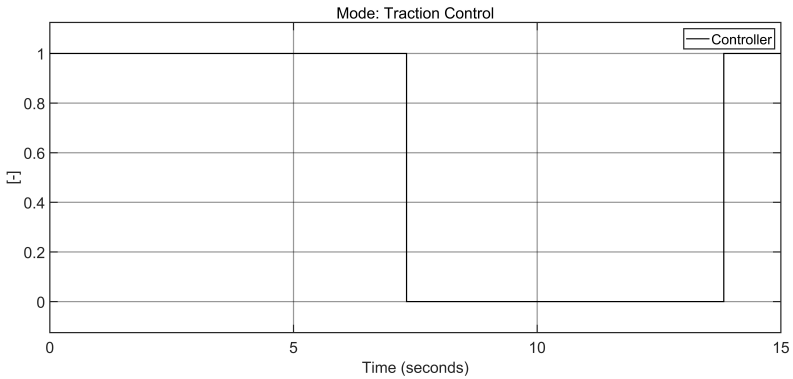


**Figure 8.18** Traction control mode with slip control on and traction control on

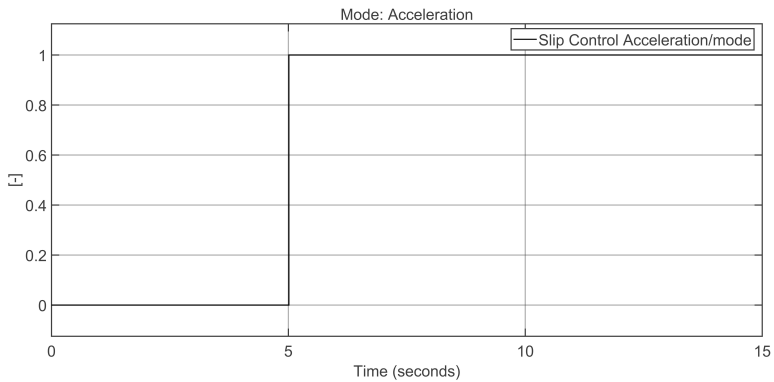


**Figure 8.19** Slip control mode with slip control on and traction control on

The simulations were carried out only focusing on acceleration situations, not braking situations. To investigate if the controllers function properly, braking simulations should also be carried out. The difference in the simulations would be a negative added torque and negative a negative slip ratio threshold.

# 9

## Implementation

In this chapter, the implementation of the current to torque conversion and the front wheel suspension are going to be explained. The implementation is different than the model as the model was developed in Matlab and Simulink, while the implementation was developed in AVR Studio and was programmed in C/C++.

### 9.1 Front Wheel Suspension

The front wheel suspension consists of two main code structures. The first one is the steady-state scenario algorithm, where the nominal lengths and values of some parts of the suspension structure are calculated, and the dynamic scenario algorithm. A distinction needs to be made between them because the former only needs to be run once when the parameters of the wheel alignment are set, while the latter needs to be running continuously. The front wheel suspension was implemented in one C file so that the calculations and the variables used were not shown in the main file. The file consisted of a series of functions. Some functions were called twice, one for each wheel, so that the code is as efficient as possible.

One function calculates the vertical load using as inputs the accelerations of the vehicle along the x-axis and the y-axis as well as the yaw rate of the vehicle to know in which direction the vehicle is turning. This information is provided by the accelerometer. The output of this function is the vertical load on each tyre.

Another function was used to calculate the steady-state information. The input of the function was the wheel-alignment parameters and the wheel (right or left) and the output of the function was the nominal lengths and dimensions of certain parts of the structure of the vehicle. This function is called twice, one for each wheel.

Another function computes the dynamic values. The inputs of the function are the vertical load of each wheel, calculated with the previous function, the steering wheel angle, provided by the steering wheel sensor (potentiometer), the outputs of the static scenario function and the wheel (right or left). The outputs of the function are the wheel angle, the camber angle and the strut length. This function is called

twice, one for each wheel. The wheel's angle values obtained are used as input for the traction control.

Lastly, another function is used to calculate the total camber angle. The camber angle is also affected by the tilt of the vehicle while cornering. The input of this function is the camber angle of each wheel and it used the yaw rate of the vehicle provided by the gyroscope to know in which direction the vehicle is turning. The output of the function is the camber angles of both wheels.

## **9.2 Current to Torque Conversion**

The implementation of the new current to torque conversion needed to be done. It was introduced as a function that provided the conversion factor when the velocity was inputted. The factor was multiplied by the current in the main code. It was done this way so that the conversion of torque to current was possible as well without the need of having extra code, just by driving the torque by the time-varying factor.

# 10

## Experiments and Results

### Front wheel suspension

To make sure that the implementation of the front wheel suspension algorithm was properly done, experiments with the real vehicle were done. To check if the data obtained is correct, the data were contrasted with the Matlab code values.

The experiments carried out consisted of making a turn with the vehicle and gathering data while doing it. The data that were desired to be analysed were the wheel's angles, the camber angles, the strut lengths, the vertical load and the steering wheel angle. The data gathered had to be filtered using a low-pass filter as it had a lot of noise. The filter used was an infinite impulse response (IRR). To check if the values were correct, the data from the vertical loads and the steering wheel angle were used as the input values to the Matlab code and the outputs were contrasted with the vehicle's data to check if they matched. By doing this, the information provided by the Matlab code should be identical or similar to the values obtained with the car. This experiment was run twice, one turning right and the second one turning left. The results shown are only from one experiment, when turning right.

When a right turn is made, the vertical force acting on the vehicle will transfer from the inner wheel (right wheel) to the outer wheel (left wheel). Figure 10.1 shows the behaviour of the vertical force on each wheel. As mentioned before, it can be seen that the load does indeed transfer from one wheel to the other. The rest of the load is acting on the rear wheel, as the vehicle was accelerating while turning. Before the vehicle was running, the static value of the vehicle vertical load on each wheel is around 1200 N, a value that is correct as it matches the calculations made using the Newton's Law and the equilibrium of forces while the vehicle was still.

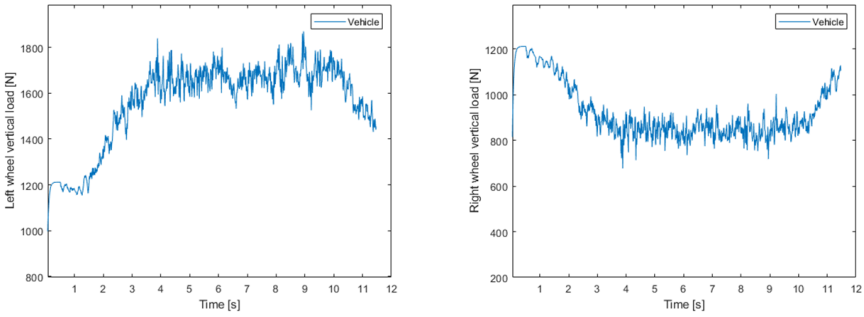


Figure 10.1 Vertical loads

Figure 10.2 shows the angle of the steering wheel while driving. The code is programmed to have positive angles when steering to the right and negative values when steering to the left. The sensor works the other way, so the data provided by the steering wheel sensor was multiplied by minus one for the computations. In the figure, it can be seen that the steering wheel has positive values, meaning the vehicle was being steered to the right.

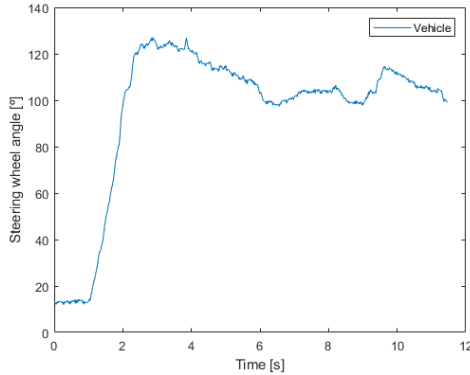
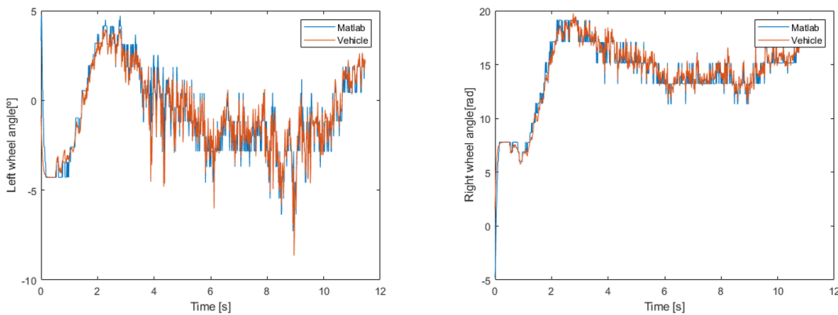


Figure 10.2 Steering wheel angle

Figure 10.3 contrasts the wheel’s angle data gathered with the vehicle and the wheel’s angle data calculated with the Matlab code when a right turn was made. If a right turn is made, the right wheel angle should increase while the left wheel angle should also increase, as the sign convention mentioned before sets. It shows that the behaviour that was expected did indeed happen. The right wheel always has a positive wheel angle, while the left wheel always has a value bigger than its nominal. It can be seen that even the filtered signals have a lot of noise. It shows that

the vehicle's information and the Matlab calculations have the same behaviour but that they are not entirely the same. This could be owing to the fact that the vehicle's information has still a lot of peaks that make the signal different from the Matlab one. It could also be because of mismatches in calculations in Matlab and the C code because of computational power. A point needs to be made about the values of the wheel's angle. It can be seen that there is a difference in the values between both wheels. With the toe angle set by OMotion, the difference should not be big, but, looking at Figure 10.3, the difference has a range of almost 15 degrees. This value is extremely high. This is because of the fact that the computations involve second-degree equations. These equations can have one, two or zero solutions. The case of zero solution is set aside, but the case of two solutions could occur. This could be the case in some calculations as these calculations are, basically, the intersection between two vectors given a starting point for each vector and the length of each vector. There could be a case where there is only one point of intersection and there could be cases where there could be two points of intersection,, as the vector are in a 3D plane. The Matlab code was designed using only one solution out of the two provided, so, in some cases, the solution provided could be the wrong one, as can be happening here. Another point needs to be made regarding the veracity of the values. Contrasting the Matlab model values versus the vehicle's values does not mean that the values are the correct ones. To know which is the real value of the wheel angle, a device should be used to measure the angles while driving or at least in a steady state, to investigate if the model does indeed copy the behaviour of the wheel's angles. OMotion has a machine in their facilities that can be used to know the real value of the wheel's angles, but because of time constraints, this validation was not done and should be done as future work.



**Figure 10.3** Wheel's angles

Figure 10.4 contrasts the camber angles data gathered with the vehicle and the camber angle data calculated with the Matlab code when a right turn was made. The right camber angle should be bigger than the left camber angle, as a right turn is made. Moreover, as a result of the inclination of the vehicle, while turning, the

right camber angle should increase when turning right while the left camber angle should decrease. It shows that the behaviour expected matches the real behaviour. The right camber angle is indeed positive and increases when turning right, while the left camber angle decreases to even more negative values. It can also be seen that there is an offset between the signals that are even more strong on the right side. This is happening because the Matlab code and the C code do not compute the camber angle with the same procedure. The C code uses the information provided by the gyroscope to know the direction of the turn, while the Matlab code, uses the height of two points to know the direction, as the information of the gyroscope is not available in the Matlab code. The C code uses an implementation that is more accurate, but the downfall is that the variable provided by the gyroscope is very sensitive. The value of the camber angle is affected by the value of the wheel angle, so the camber angle values would change when this issue is fixed.

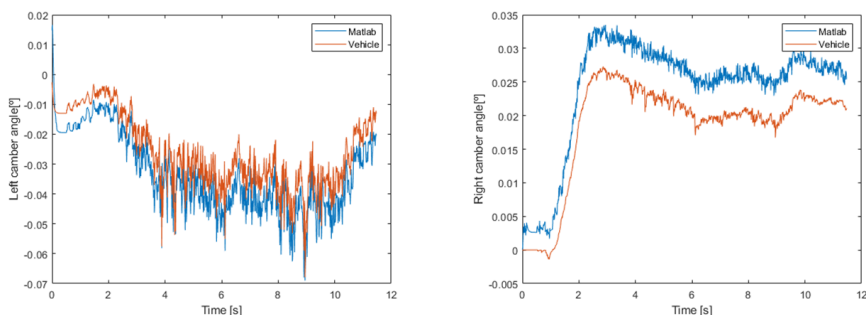
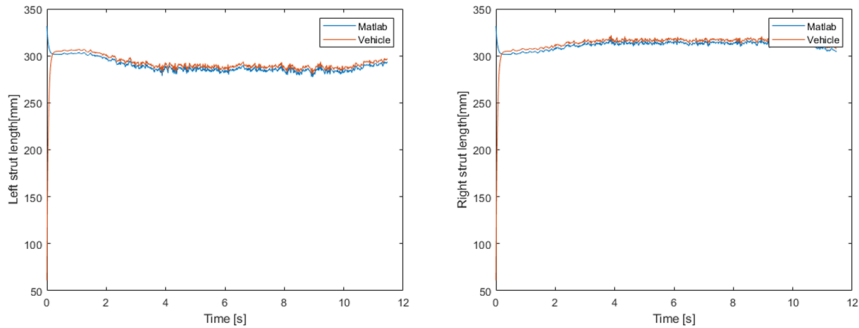


Figure 10.4 Camber angles

Figure 10.5 contrasts the strut lengths data gathered with the vehicle and the strut lengths data calculated with the Matlab code when a right turn was made. The behaviour of the strut should work as follow: when a nominal vertical load is acting on the wheel, the strut should have the nominal length. When a tyre has more force acting on it than the nominal, the force acting on the strut increases and the length of the strut decreases. When a tyre has less force acting on it than the nominal, the force acting on the strut decreases and the length of the strut increases. So, when making a right turn, the force acting on the right wheel decreases, making the right strut length bigger than the nominal and the force acting on the left wheel increases, making the left strut length smaller than the nominal. It shows that the behaviour expected does indeed match the real behaviour of the strut length. The left strut is smaller than the nominal value while the right strut is bigger than the nominal value when a right turn is made. A point needs to be made regarding the veracity of the values. As it was done with the angles of the wheels, the procedure for the strut lengths is to compare the model values with the implementation values. To be sure



that the results are the correct ones, a device should be used to measure the variation of the spring of the strut while driving.



**Figure 10.5** Strut lengths

When a left turn was made, the behaviour of the results was also the ones that was expected. Regarding the wheel's angles, their values were mostly negative, as was expected. Regarding the camber angles, the behaviour was the expected one but the signals also presented the offset that can be seen in Figure 10.4. Regarding the strut lengths, while turning left, the right strut length became smaller because the vertical force acting on the tyre is bigger than the nominal, while the left strut length became bigger, as the vertical force acting on the tyre is smaller than the nominal.

## Slip control

Experiments with the real vehicle were carried out to evaluate the performance of the implemented code with the current to torque conversion and the thresholds. During these experiments, the slip ratio behaved strangely. The experiments consisted of driving the vehicle and saving data while driving. The data that were stored were the slip ratio calculated by the C code implemented in the vehicle. The slip ratio thresholds for this experiment were set to 0.1 for acceleration and -0.1 for braking. It was seen in the experiments that the slip ratio thresholds were not symmetrical. The slip ratio curve seems to have the proper behaviour but it is offset downwards. This could be because of the fact that the radius that is used to calculate the slip ratio is not accurate as its value depends on many factors, such as vertical load, pressure on the wheels and the wear of the tyre. To compensate for this issue, the slip ratio thresholds were lowered. The acceleration slip threshold was set to 0.1, while the braking threshold was set to -0.15. Figure 10.6 shows the value of the slip ratio calculated by the C-code implemented in the vehicle. Figure 10.7 shows the motor's current during the same experiment. The behaviour that was expected was the following: when the current is positive, the vehicle is being accelerated. When

the current turns to -150 the brakes have been applied. When the vehicle is accelerated, the slip ratio should be positive, while it should be negative when the vehicle is braking. This is not the case, as it can be seen when the figures are contrasted that the slip ratio is negative even though the vehicle is being accelerated. If the value of the radius of the vehicle was increased 5%, the slip ratio calculated by the vehicle moved to more expected values. The calculations of the slip ratio are very sensitive, so a correct identification of the wheel radius is very important.

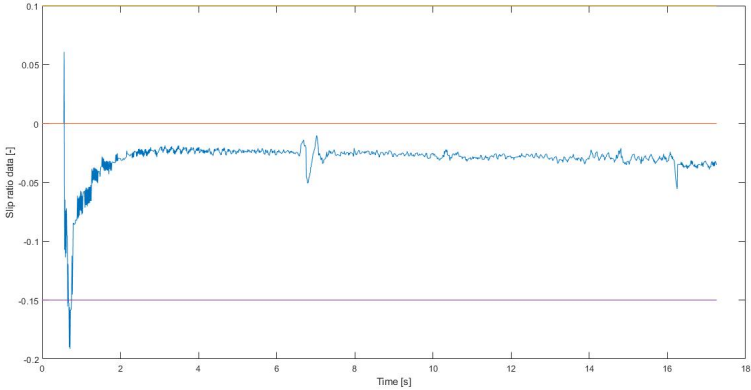


Figure 10.6 Slip ratio provided by vehicle

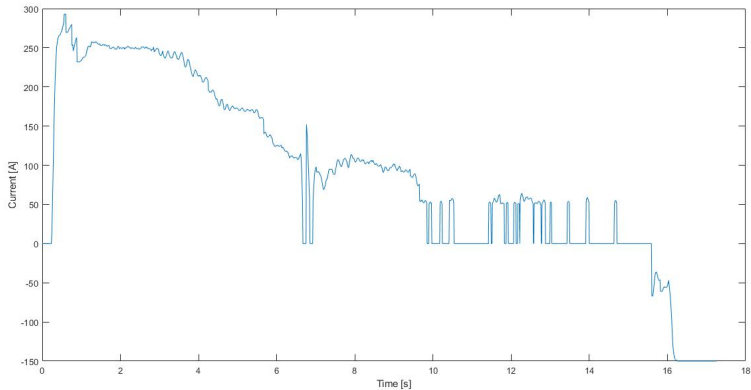


Figure 10.7 Motor current of the vehicle

# 11

## Conclusion

The aim of this chapter is to provide the conclusion extracted from the work that was carried out and the results obtained, relating the results to the objectives that were set at the beginning of the Master Thesis in Chapter 1.

- The controllers were integrated and simulations were carried out to prove that the integration performance was the expected. The tuning of the different control parameters was not achieved because of time constraints as well as model inaccuracies. The control logic parameters for the slip control were modified while the control logic parameters for the traction control were left untouched. In the simulations, it was seen that the integration of the controllers behaved as it was expected. The implementation of this integration in the vehicle was not achieved. Real-vehicle experiments evaluating the integration of the controllers were not carried out because of time constraints and should be done in the future. Experiments were carried out to test the slip control with the new updates and new device tuning. During these experiments, it was noticed that the slip ratio calculations were not the expected ones, so the control logic parameters were changed to compensate this error.
- The automatic approach to calculate the wheel's angles was designed and implemented in the vehicle. The implementation was tested and analysed, checking if the results of the implementation code matched the results of the Matlab code, when the inputs were the same. It was concluded that the procedure has the expected behaviour. There are some cases that the results do not match entirely because of the fact that the implementation code and the Matlab code used different approaches to calculate the same data. The results were not validated with devices to check their veracity. To validate the results, machines, devices or sensors need to be used to acquire the real data and contrast it with the previous results.
- The conversion of current to torque was developed and implemented in the vehicle. The assumption that the conversion factor was affected by the velocity was shown to be true.

- The devices that were tuned throughout the Master Thesis were the gyroscope and accelerometer, the ABS and the steering wheel sensor. The tuned parameters were implemented in the vehicle. The new cornering and longitudinal stiffness parameters were also implemented in the model as well as other parameters that also needed to be tuned as a result of small modifications that the vehicle had underwent during the past year.
- A solution to solve the difficult tuning of the traction control was not investigated because of time constraints. The approach that could be used is to design a real-time identification and parameter estimation to the system or to design an adaptation of the parameters of the controller using strategies such as gain scheduling, with manual mode selection by the driver.

## 11.1 Future Work

As mentioned before, the model used to represent the behaviour of the vehicle does not match the behaviour the vehicle has under the same conditions. The model needs further investigation. Other approaches could be used, such as the Magic Formula, or the calculation of the forces could be done following [Rajamani, 2012b] guidelines.

As mentioned in Chapter 10, the validation of the results of the front wheel suspension experiments needs to be done. To know the real value of the wheel angle, a device should be used to measure the angles while driving or at least in a steady state, to see if the model does indeed mimic the behaviour of the wheel's angles. OMotion has a machine in their facilities that can be used to measure the actual value of the wheel's angles while the vehicle is still. The same procedure needs to be done with the strut's lengths. To know the real values, a device should be used to measure the length of the spring of the strut while driving. Also, the length of the strut in steady-state could be measured with the device to evaluate if both the dynamic-state and the steady-state calculations represent the strut correctly.

As stated in Chapter 10, a more accurate estimation of the wheel radius should be investigated to obtain the slip ratio values with higher accuracy. Moreover, the tuning of the control parameters needs to be done and experiments should be run to test the performance of the controllers while driving.

# Bibliography

- Aly, Zeidan, Hamed and Salem (2011). “An antilock-braking systems (abs) control: A technical review”. *Intelligent Control and Automation*. **2**, pp. 186–195.
- Athans (1978). *The role of modern control theory for automotive engine control*. Tech. rep. 780852. SAE Technical Paper., p. 5.
- Autodesk (2022). *Autocad*. Version 2020.
- Crouch, R. and C. Haines (2004). “Mathematical modelling: Transitions between the real world and the mathematical model”. *International Journal of Mathematical Education in Science and Technology* **35**:2, pp. 197–206.
- Decker, Emig and Schramm (1987). “Traction control (ASR) for commercial vehicles, a further step towards safety on our roads”. *SAE Transactions*. **96**, pp. 1549–1556.
- Dugoff, F. and Segel (1969). *Tire Performance Characteristics Affecting Vehicle Response to Steering and Braking Control Inputs*. Tech. rep. 00223094. Highway Safety Research Institute at The University of Michigan, Ann Arbor, Michigan.
- Friedrich (2014). “Basic principles of vehicle dynamics”. In: *Fundamentals of Automotive and Engine Technology: Standard Drives, Hybrid Drives, Brakes, Safety Systems*. Springer Fachmedien Wiesbaden., pp. 114–129.
- Furferi, Governi, Volpe and Carfagn (2013). “Design and assessment of a machine vision system for automatic vehicle wheel alignment”. *International Journal of Advanced Robotic Systems* **10**:5, p. 242.
- Gillespie (1992). *Fundamentals of vehicle dynamics*. Revised Edition. SAE International.
- Jalali, Khajepour, Chen and Litkouhi (2016). “Integrated stability and traction control for electric vehicles using model predictive control”. *Control Engineering Practice*. **54**, pp. 256–266.
- Jo, You and Joeng (2008). “Vehicle stability control system for enhancing steerability, lateral stability, and roll stability.” *International Journal of Automotive Technology* **9**:571.

## Bibliography

- Kachroo and Tomizuka (1994). "Vehicle traction control and its applications". *UC Berkeley: California Partners for Advanced Transportation Technology*.
- Karlin (2021). *Slip Control for a Three-Wheeled Electric Motorcycle*. MA thesis. Lund University, TFRT-6128.
- Kawabe (2012). "Model predictive PID traction control systems for electric vehicles". *2012 IEEE International Conference on Control Applications.*, pp. 112–117.
- Lateral and Longitudinal Load Transfers* (2022). Accessed: 2022-04-25. URL: <https://suspensionsecrets.co.uk/lateral-and-longitudinal-load-transfer/>.
- MathWorks (2022). *Matlab and simulink*. Version R2020a.
- Microchip (2022). *Microchip studio for avr*. Version 7.0.2542.
- Nations, U. (202). *Sustainable development goals*. Accessed: 2022-06-08. URL: <https://sdgs.un.org/>.
- Nilsson and Sandstedt (2021). *Traction Control of a Three-Wheeled Electric Motorcycle*. MA thesis. Lund University, TFRT-6138.
- OMotion (2021). *Technical specifications*. Accessed: 2022-06-25. URL: <https://omotion.se/>.
- Pacejka (2012). *Tire and Vehicle Dynamics*. 3rd ed. Butterworth-Heinemann.
- Pundir (2019). "Review paper on an automatic wheel alignment system to overcome from wheel alignment issues". *International Journal of Aerospace and Mechanical Engineering* **6**:2, p. 4.
- Rajamani (2012a). "Electronic stability control". In: *Vehicle Dynamics and Control*. Springer.
- Rajamani (2012b). "Vehicle dynamics". In: *Vehicle Dynamics and Control*. 2nd ed. Springer.
- Simon Tatham (2022). *Putty*. Version 0.76.
- Urda, Cabrera, Castillo and Guerra (2016). *The Dynamics of Vehicles on Roads and Tracks*. 1st ed. CRC Press.

# A

## Nomenclature

**Table A.1** Nomenclature I

| Abbreviation                         | Name  |
|--------------------------------------|---|
| $g$                                  | Gravity   |
| $F_{xfr}, F_{xfl}, F_{xr}$           | Longitudinal force of front rear wheel, front left wheel and rear wheel |
| $F_{yfr}, F_{yfl}, F_{yr}$           | Lateral force of front rear wheel, front left wheel and rear wheel      |
| $F_{zfr}, F_{zfl}, F_{zr}$           | Vertical force of front rear wheel, front left wheel and rear wheel     |
| $F_d$                                | Drag force  |
| $F_{rr}$                             | Rolling resistance force  |
| $F$                                  | Normalized force  |
| $X, Y, Z$                            | Global coordinates of vehicle   |
| $\dot{x}, \dot{y}, \dot{z}$          | Velocity along the x, y and z axis of the vehicle                       |
| $\ddot{x}, \ddot{y}, \ddot{z}$       | Acceleration along the x, y and z axis of the vehicle                   |
| $\ddot{x}_m, \ddot{y}_m, \ddot{z}_m$ | Acceleration along the x, y and z axis of the accelerometer             |
| $m$                                  | Mass of the vehicle   |
| $h$                                  | Height of the COG   |
| $h_d$                                | Height of drag force  |
| $\delta_{fr}, \delta_{fl}, \delta_r$ | Right, left and rear wheel angle  |
| $\sigma_{fr}, \sigma_{fl}, \sigma_r$ | Right, left and rear wheel slip ratio                                   |
| $\alpha_{fr}, \alpha_{fl}, \alpha_r$ | Right, left and rear wheel slip angle                                   |
| $C_r$                                | Rolling resistance coefficient  |
| $\rho$                               | Air density   |
| $A$                                  | Frontal area of the vehicle   |
| $C_d$                                | Drag coefficient  |
| $\mu$                                | Friction coefficient  |
| $\bar{\sigma}$                       | Normalized longitudinal slip ratio                                      |
| $\bar{\alpha}$                       | Normalized lateral slip ratio   |
| $\bar{\sigma}_r$                     | Normalize slip ratio  |
| $C_\sigma$                           | Cornering stiffness coefficient   |
| $C_\alpha$                           | Longitudinal stiffness coefficient                                      |

**Table A.2** Nomenclature II

| Abbreviation      | Name   |
|-------------------|--|
| $I_{wf}, I_{wr}$  | Front and rear wheel momentum of inertia                         |
| $\tau$            | Torque   |
| $\tau_{bf}$       | Front wheels braking torque                                      |
| $\tau_{br}$       | Rear wheel braking torque  |
| $r_f$             | Front wheels radius  |
| $r_r$             | Rear wheel radius  |
| $w$               | Yaw rate   |
| $\dot{w}$         | Angular acceleration   |
| $c$               | Percentage of total force  |
| $a_x, a_y$        | Acceleration along the x and y axis                              |
| $L$               | Wheel base   |
| $l_w$             | Track width  |
| $\ddot{\Theta}$   | Vehicle's pitch acceleration                                     |
| $\ddot{\Phi}$     | Vehicle's roll acceleration                                      |
| $\ddot{\Psi}$     | Vehicle's yaw acceleration                                       |
| $\ddot{\Theta}_m$ | Gyroscope's pitch acceleration                                   |
| $\ddot{\Phi}_m$   | Gyroscope's roll acceleration                                    |
| $\ddot{\Psi}_m$   | Gyroscope's yaw acceleration                                     |
| $\chi$            | ABS factor   |
| $n$               | Number of tests  |
| $I$               | Current  |
| $s$               | Slope  |
| $q$               | Y-intercept  |
| $T_d$             | Driver's torque  |
| $T_c$             | Controlled torque  |
| $l_f$             | Distance to center of gravity of the vehicle from the front axle |
| $l_r$             | Distance to center of gravity of the vehicle from the rear axle  |



# B

## Sustainable Development Goals

In September 2015, world leaders agreed to set goals that needed to be met in the next 15 years with the aim of ending poverty throughout the world, ending hunger, guaranteeing a healthy life for citizens, guaranteeing quality education, achieving gender equality, ensure clean water and sanitation globally, use sustainable energy, promote economic growth and decent work, end inequalities, achieve sustainable cities, produce and consume responsibly, take action against climate change, protect and conserve underwater life and terrestrial ecosystems, promote just and peaceful societies and finally create alliances to achieve these goals [Nations, 0202]. All of them are shown in Figure B.1.



**Figure B.1** Sustainable development goals. Photo: United Nations

## *Appendix B. Sustainable Development Goals*

The main objective pursued by this project is to improve the performance of an electric vehicle so that it becomes safer to drive around with it. This aligns with objective number 3, as it is trying to avoid as much danger as possible while driving a car. Furthermore, objectives number 7 and 13 have an important impact in this Master Thesis as the vehicle that is worked with is a totally electric vehicle. Objective number 9 is also being accounted for, as control theory is a common methodology used in the automotive industry used to improve the performance and to improve safety for drivers.

|  |                                       |   |             |
|--|---------------------------------------|---|-------------|
| <b>Lund University</b><br><b>Department of Automatic Control</b><br><b>Box 118</b><br><b>SE-221 00 Lund Sweden</b>   |                                       | <i>Document name</i><br><b>MASTER'S THESIS</b>  |             |
|  |                                       | <i>Date of issue</i><br><b>August 2022</b>  |             |
|  |                                       | <i>Document Number</i><br><b>TFRT-6182</b>  |             |
| <i>Author(s)</i><br><b>Blanca Zumárraga</b>  |                                       | <i>Supervisor</i><br><b>Ola Svensson, OMotion AB</b><br><b>Björn Olofsson, Dept. of Automatic Control, Lund University, Sweden</b><br><b>Anders Robertsson, Dept. of Automatic Control, Lund University, Sweden</b><br><b>Tore Hägglund, Dept. of Automatic Control, Lund University, Sweden (examiner)</b> |             |
| <i>Title and subtitle</i><br><b>Implementation and integration of slip and traction controllers for a three-wheel electric vehicle</b>   |                                       |   |             |
| <i>Abstract</i><br><p>The purpose of the Master Thesis is, on one hand, to develop a traction control system, integrating and implementing two controllers in the vehicle, each of them previously designed and tested separately, to test them together to evaluate their performance. On the other hand, to develop accurate and well-performing controllers, the data acquisition needs to be precise so parameters and devices need to be tuned again, because of small modification in the structure of the vehicle. Parameters such as the cornering and longitudinal stiffness were studied to have more faithful simulations, and devices such as the gyroscope and the ABS were tuned. Moreover, along the lines of acquiring accurate data, another purpose of the Master Thesis is to develop procedures or algorithms to acquire data using automated approaches, instead of the manual approaches that were used previously, specifically concerning the wheel's angles.</p> <p>A mathematical representation of the vehicle dynamics, developed by [Nilsson and Sandstedt, 2021], is used to simulate the performance of the controllers and to tune them accordingly. Simulations were carried out to test the integration of the controllers and evaluate their performance. The controllers behaved according to the expectations and performed accurate simulations. The controllers should then be implemented in the real vehicle to confirm that their performance is the desired.</p> <p>The data acquired provided information of each of the studied parameters and they showed that the procedure developed to obtain the wheel's angles was properly implemented. The devices that needed tuning were properly tuned. The model parameters were updated with new values so that the model represented the real system as well as possible.</p> |                                       |   |             |
| <i>Keywords</i>  |                                       |   |             |
| <i>Classification system and/or index terms (if any)</i>   |                                       |   |             |
| <i>Supplementary bibliographical information</i>   |                                       |   |             |
| <i>ISSN and key title</i><br><b>0280-5316</b>  |                                       |   | <i>ISBN</i> |
| <i>Language</i><br><b>English</b>  | <i>Number of pages</i><br><b>1-80</b> | <i>Recipient's notes</i>  |             |
| <i>Security classification</i>   |                                       |   |             |

<http://www.control.lth.se/publications/>